Accepted Manuscript

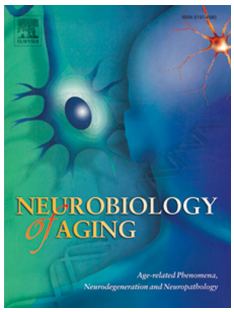

Functional signature of conversion of Mild Cognitive Impairment patients

Stefano Delli Pizzi, Miriam Punzi, Stefano L. Sensi

PII: S0197-4580(18)30367-1

DOI: 10.1016/j.neurobiolaging.2018.10.004

Reference: NBA 10398

To appear in: *Neurobiology of Aging*

Received Date: 1 April 2018

Revised Date: 24 September 2018

Accepted Date: 4 October 2018

Please cite this article as: Pizzi, S.D., Punzi, M., Sensi, S.L, for the Alzheimer's Disease Neuroimaging Initiative, Functional signature of conversion of Mild Cognitive Impairment patients, *Neurobiology of Aging* (2018), doi: https://doi.org/10.1016/j.neurobiolaging.2018.10.004.

Functional signature of conversion of Mild Cognitive Impairment patients

Stefano Delli Pizzi [1,2], Miriam Punzi [1,2], Stefano L Sensi [1,2,3], for the Alzheimer's Disease Neuroimaging Initiative*

[1] *Department of Neuroscience, Imaging and Clinical Sciences, "G. d'Annunzio" University, Chieti, Italy;*

[2] *Center for excellence on Aging and Translational Medicine - Ce.S.I. - Me.T., "G. d'Annunzio" University, Chieti, Italy;*

[3] *Departments of Neurology and Pharmacology, Institute for Memory Impairments and Neurological Disorders, University of California-Irvine, Irvine, CA, USA.*

**Data used in the preparation of this article were obtained from the Alzheimer's Disease Neuroimaging Initiative (ADNI) database (adni.loni.usc.edu). As such, the investigators within the ADNI contributed to the designed and implementation of ADNI and/or provided data but did not participate in analysis or writing of this report. A complete listing of ADNI investigators can be found at: http://adni.loni.usc.edu/wp-content/uploads/how_to_apply/ADNI_Acknowledgement_List.pdf*

Corresponding author
Stefano L. Sensi, MD, PhD
Molecular Neurology Unit
Center of Excellence on Aging and Translational Medicine (CeSI-MeT)
University "G. d'Annunzio", Chieti-Pescara
Via Luigi Polacchi 11, 66100, Chieti, Italy
Phone number: +39 0871 541544
Fax number: +39 0871 541542
E-mail: ssensi@uci.edu

Running title: Functional connectivity signature in MCI

Abstract

The entorhinal-hippocampal circuit is a strategic hub for cognition and the first site affected by Alzheimer's Disease (AD). We investigated MRI patterns of brain atrophy and functional connectivity in an ADNI dataset that included healthy controls, Mild Cognitive Impairment (MCI), and AD subjects. MCI individuals were clinically evaluated 24 months after the first MRI scan, and the cohort subdivided into sets of individuals who either did (c-MCI) or did not (nc-MCI) convert to AD. The MCI group was also divided into patients who did show (MCI^{AD+}) or not (MCI^{AD-}) the presence of AD-related alterations in the liquor. AD patients exhibited the collapse of the long-range hippocampal/entorhinal connectivity, pronounced cortical/sub-cortical atrophy, and a dramatic decline in cognitive performances. c-MCI or MCI^{AD+} patients showed memory deficits, entorhinal/hippocampal hypo-connectivity, and concomitant atrophy of the two regions. nc-MCI or MCI^{AD-} subjects had no atrophy but showed hippocampal/entorhinal hyper-connectivity with selected neocortical/sub-cortical regions involved in memory processing and brain meta-stability. This hyper-connectivity may represent a compensatory strategy against the progression of cognitive impairment.

Keywords: Alzheimer's Disease; cerebellum; entorhinal cortex; functional connectivity; hippocampus; GABA; excitotoxicity.

Abbreviations

$A\beta_{1-42}$=amyloid β_{1-42}; AD=Alzheimer's Disease; ADAS=Alzheimer's Disease Assessment Scale; ADNI=Alzheimer's Disease Neuroimaging Initiative; ADRDA=Alzheimer's Disease and Related Disorders Association; AF=Animal Fluency; AVDELT= Rey Auditory Verbal Learning Test-Delayed Recognition Score; AVDEL30=Rey Auditory Verbal Learning Test-Delayed 30 Minute Delay Total; BNT=Boston Naming Test; BOLD=Blood Oxygen Level Dependent; CDR-RS=Clinical Dementia Rating Scale; c-MCI=MCI patients who convert to AD; DMN=Default-Mode Network; EC=entorhinal cortex; EPI=Echo-planar imaging; eTIV=estimated total intracranial volume; FC=functional connectivity; FAQ=Functional Activities Questionnaire; GM=grey matter; HC=healthy controls; HP=Hippocampus; LDEL=Logical Memory-Delayed Recall Total Number of Story Units Recalled; LIMM=Logical Memory-Immediate Recall Total Number of Story Units Recalled; MCI=Mild Cognitive Impairment; MCI^{AD+}=MCI subjects who showed presence of AD-related alterations in the CSF; MCI^{AD-}=MCI subjects who did not show presence of AD-related alterations in the CSF; MMSE=Mini-Mental State Examination; MNI=Montreal Neurological Institute; MoCA=Montreal Cognitive Assessment; mPFC=medial prefrontal cortex; NA=Not Applicable; nc-MCI=patients with Mild Cognitive Impairment who remained stable in their diagnosis of or who returned to be healthy; NINCDS=National Institute of Neurologic and Communicative Disorders and Stroke; PMN=posterior medial network; p-Tau_{181}=tau phosphorylated at threonine 181; RAVLT=Rey Auditory Verbal Learning Test; rs-fMRI=Resting-state functional Magnetic Resonance Imaging; TMT=Trail Making Test; t-Tau=total tau; WM=white matter; WMS-R=Wechsler Memory Scale-Revised.

1. Introduction

Brain aging and aging-related neurodegenerative disorders are a significant health challenge for contemporary societies. Brain aging represents a favorable background for the onset and development of neurodegeneration and dementia. Alzheimer's Disease (AD) is a condition associated with the development of irreversible cognitive and behavioral deficits and preceded by a prodromal stage known as Mild Cognitive Impairment (MCI). MCI patients do not fulfill the diagnostic criteria for dementia but show significant cognitive deficits that mostly occur in mnemonic domains (Petersen et al. 2010). MCI subjects progress to AD in 60-65% of cases (Busse et al. 2006) with a conversion rate that reaches 8.1% per year (Mitchell and Shiri-Feshki 2009). Thus, the early identification of the brain changes associated with MCI is critical to catch the disease at its initial stage, unravel its pathogenic mechanisms, and help the design of more effective therapeutic interventions.

Neuroimaging approaches have been extensively employed to detect the initial changes associated with the early stages of AD (Frisoni and Jessen 2018). Resting-state functional Magnetic Resonance Imaging (rs-fMRI) is a non-invasive tool that allows the investigation of the operational changes and network reconfigurations that occur in several neurological/neurodegenerative conditions, including AD. In MCI patients, rs-fMRI has been successfully employed in the quest to detect abnormalities in the brain functional connectivity that occur before the appearance of patent signs of structural damage (Badhwar et al. 2017, Drzezga et al. 2011, Canuet et al. 2015).

The entorhinal-hippocampal circuit is a strategic region for the control of cognitive processes and the first site to be affected by the AD-related pathology (Braak et al. 2013, Gomez-Isla et al. 1996). In the AD brain, early signs of synaptic degradation occur within the perforant path, neurodegeneration then spreads to the layers II-III of the entorhinal cortex, the hippocampal CA1 subfield, the subicular areas, ultimately affecting the whole hippocampus (Mueller et al. 2010; Wolk et al. 2011; Yushkevich et al. 2015). This sequence is crucial as the entorhinal-hippocampal complex plays an essential role in the processing of long-term memory (Preston and Eichenbaum 2013). Functional changes in the hippocampus and, in particular, the CA3/dentate regions have been associated with the occurrence of episodic memory deficits that develop upon physiological aging as well as MCI (Yassa et al. 2010a, 2011). Moreover, the hippocampus plays a role in maintaining the brain system stability and promotes the adaptive recalibration of network functioning observed in response to pathological stressors (van den Heuvel and Sporns 2011, Hillary and Grafman 2017).

In this study, we investigated, in a cohort of one hundred thirty-five individuals, differences in structural MRI (sMRI) and rs-fMRI features that occur within the cortico-hippocampal and cortico-

entorhinal circuits. The study group included Healthy Control (HC) (n=40), MCI (n=67), and AD (n=28) subjects. The dataset also provided information on the demographic, neuropsychological/clinical, APOE status, and the CSF levels of AD-related pathogenic proteins like the amyloid β_{1-42} peptide ($A\beta_{1-42}$), tau phosphorylated at threonine 181 (p-Tau_{181}), and the ratio of p-Tau_{181}/$A\beta_{1-42}$.

sMRI data were employed to investigate differences in brain volumes and cortical thickness among the study participants. Rs-fMRI data were used to evaluate differences in the functional connectivity (FC) occurring in the circuits linking the hippocampus or the entorhinal cortex to the cortex. The progression or clinical stability of HC or MCI subjects was assessed by using clinical follow-up data obtained 24 months after the initial MRI session. These longitudinal data were instrumental to divide the MCI group into two subsets: patients who converted (c-MCI) or did not convert (nc-MCI) to AD. As not all the MCI symptoms are necessarily dependent on the presence on underlying AD pathology, it is conceivable that some nc-MCI subjects are protected from the AD conversion mainly because of the absence of significant levels of amyloid- or tau-related pathology. Conversely, compared to MCI with low levels of amyloid and tau, MCI subjects with high levels of these molecular AD determinants are likely to convert with higher frequency (Jack et al. 2016; Johnson et al. 2016). Thus, to explore this issue, in a subsequent analysis, we also subdivided our MCI sample in MCI^{AD+} or MCI^{AD-} by taking in consideration the presence of an AD-related CSF biomarker, the p-Tau_{181}/ $A\beta_{1-42}$ ratio, a value that can be used as a proxy of ongoing pathology.

The overall aim of the study was to unravel a functional biomarker, centered on the FC of the hippocampus and entorhinal cortex, that can be employed to identify MCI subjects who are more likely to convert to AD. As altered synaptic activation and plasticity participate in shaping the course of the disease, we tested whether nc-MCI patients, among other factors, maintain their cognitive status trough an underlying adaptive hyper-connectivity that takes place between the hippocampus and the neocortical/sub-cortical regions that are strategic for memory processing and brain meta-stability. We also tested whether c-MCI and AD subjects diverge from nc-MCI in terms of structural and functional changes that correlate with the decline of the cognitive performances. Finally, given the role of amyloid and tau-driven pathology in the modulation of neurodegeneration, we also evaluated how the presence of these proxy indices of AD-related pathology affects the connectivity patterns of the MCI^{AD+} and MCI^{AD-} subgroups.

2. Materials and methods

2.1 Experimental design

Data employed for this article were obtained from the ADNI-GO/2 database. ADNI was launched in 2003 as a public-private partnership led by Michael W. Weiner. The primary goal of ADNI is to employ serial MRI, PET, biological markers, and clinical and neuropsychological data to investigate the features of patients affected by the AD spectrum. For up-to-date information on the initiative, see www.adni-info.org.

Experiments fulfilled the ethical standards and the Declaration of Helsinki (1997) and subsequent revisions. Informed consent was obtained from study participants or authorized representatives. Study participants had a good general health status and no diseases expected to interfere with the study. Overall, the ADNI-GO/2 database included one hundred seventy participants who have completed the 3T-sMRI and 3T-rs-fMRI. The age range was between 57 and 88 years old.

Participants who did not complete a clinical follow-up, performed 24 months after the first MRI session, or those who showed the presence of technical issues related to their MRI raw-data (i.e., artifacts, dis-homogeneity in acquisition parameters, images deformed for missing information raw-file) were excluded from the study sample (**Suppl. Fig. 1**). Our final sample included one hundred thirty-five participants divided into forty HC subjects, sixty-seven MCI patients, and twenty-eight AD patients. Based on the clinical follow-up, the MCI group was further subdivided into a group of fifty-four nc-MCI patients and thirteen c-MCI patients. Our MCI sample was also subcategorized taking into account the CSF levels of AD-related biomarkers. Using a cut-off of 0.0198 for the p-Tau_{181}/$A\beta_{1-42}$ ratio (Schindler et al. 2018), the MCI group as well as the nc-MCI subset was divided into subjects positive [(MCI^{AD+}(n=37) or nc-MCI^{AD+}(n=25)] or negative [(MCI^{AD-} (n=22) or nc-MCI^{AD-}(n=21)] for AD pathology (**Suppl. Fig. 2**).

2.2 Neuropsychological assessment

All subjects underwent clinical and cognitive evaluations at the time of the MRI scan. The ADNI neuropsychological dataset includes the Mini-Mental State Examination (MMSE) (Folstein et al. 1975) and the Montreal Cognitive Assessment (MoCA) (Nasreddine et al. 2005) to investigate global cognition; the Functional Activities Questionnaire (FAQ) for the assessment of daily living activities (Pfeffer et al. 1982); the Alzheimer's Disease Assessment Scale-Cognitive subscales (ADAS - 11 items scores; ADAS - 13 items scores) to evaluate the severity of impairments of memory, learning, language (production and comprehension), praxis, and orientation (Mohs and Cohen 1988; Mohs et al. 1997); the Animal Fluency (AF) (Morris et al. 1989) and the 30-item Boston Naming Test (BNT) (Kaplan et al. 1983) to investigate semantic memory and language abilities; the Trail Making Test (TMT), part A and B (time to completion) to assess attention/executive functions (Spreen 1998); the Rey Auditory Verbal Learning Test and Logical

Memory II, subscale of the Wechsler Memory Scale-Revised (WMS-R) to investigate recall and recognition (Rey 1964; Wechsler 1987).

HC subjects were free of memory complaints and without significant impairment as far as general cognitive functions or performance in daily living activities. The inclusion criteria for HC subjects were: MMSE scores between 24 and 30, a global score of 0 on the Clinical Dementia Rating Scale (CDR-RS; Morris JC 1993), and a score above the cutoff level on the WMS-R Logical Memory II (≥3 for 0-7 years of education, ≥5 for 8-15 years of education, and ≥9 for 16 or more years of education).

The inclusion criteria for MCI patients were: MMSE scores between 24 and 30, memory impairments identified by the partner, with or without complaints by the participant, a CDR score of 0.5, and memory deficits as indicated by scores below the cutoff level on the WMS-R Logical Memory II (3-6 for years of education 0-7 , 5-9 for 8-15 years of education, and ≤9 for >15 years of education). The subject general cognition status and functional performances were sufficiently preserved to exclude a diagnosis of AD.

AD patients fulfilled the criteria of probable AD set by the National Institute of Neurologic and Communicative Disorders and Stroke (NINCDS) as well as the Alzheimer's Disease and Related Disorders Association (ADRDA). AD patients had MMSE scores between 20 and 26 and CDR-RS between 0.5 and 1.0.

2.3 CSF and APOE genotyping

CSF data were available for 87.4% of the total sample. The set included information on levels of the $A\beta_{1-42}$, total tau (t-Tau), and p-Tau_{181}. Highly standardized $A\beta_{1-42}$, t-Tau and p-Tau_{181} levels were measured using the Roche automated immunoassay platform (Cobas e601) and immunoassay reagents. Details on the methods for the acquisition and measurement of CSF are reported in the ADNI website (http://www.adni-info.org). The apolipoprotein E (APOE) ε4 allele frequency was also investigated at the screening stage.

2.4 MRI acquisition protocol

MR data were all acquired with a Philips 3T scanner (see details at http://adni. loni. usc. edu/wp-content/uploads/2010/05/ADNI2_MRI_Training_Manual_FINAL.pdf), thereby limiting bias and technical issues associated with the use of different scanner types/brands. T_1-weighted images were obtained using 3D Turbo Field-Echo sequences (TFE, Slice Thickness=1.2 mm; TR/TE=6.8/3.1 ms). One run of Resting-state Blood Oxygen Level Dependent (BOLD) fMRI data was acquired using gradient-echo T_2*-weighted echo-planar (EPI) sequence (in-plane voxel size=3.3125 mm x 3.3125 mm, slice thickness

3.3125 mm, and TR/TE=3000/30 ms. Subjects were instructed to lay still and keep their eyes open during acquisition.

2.5 MRI data analysis

FreeSurfer (version 6.0) was employed to perform sMRI and rs-fMRI data analysis. For each study participants, T_1-weighted images were analyzed using the "recon-all -all" command line to obtain the automated reconstruction and labeling of cortical and subcortical regions (Fischl et al. 2004). The pre-processing steps encompassed magnetic field inhomogeneity correction, affine-registration to Talairach Atlas, intensity normalization and skull-strip. The processing steps involved segmentation of the subcortical white matter (WM) and deep grey matter (GM) volumetric regions, tessellation of the GM and WM matter boundary, automated topology correction, surface deformation following intensity gradients to optimally position the GM and WM and GM/cerebrospinal fluid borders at the location where the greatest shift in intensity delineates the transition to the other tissue class. The total volume of the left and right hippocampi and the estimated total intracranial volume (eTIV) were calculated using the "asegstats2table". The hippocampal volumes were normalized with a ratio obtained by dividing hippocampal volumes by eTIV. The left and right masks of the hippocampi and entorhinal cortices were obtained by the "recon-all -all" command lines and used as "seed regions" for FC analysis using FreeSurfer - Functional Analysis Stream (http://surfer.nmr.mgh.harvard.edu/fswiki/FsFastFunctionalConnectivityWalkthrough). The ''preproc-sess'' command line was employed to perform motion and slice timing corrections, masking, registration to the structural image, sampling to the surface, surface smoothing by 5 mm, and sampling to the MNI305 with volume smoothing. Surface sampling of time-series data was carried out onto the surface of the left and right hemispheres of the "fsaverage" template of FreeSurfer. Nuisance regressors were obtained for each study participants by extracting the EPI average time courses within the ventricle mask and the white matter mask (taking into consideration the top 5 principal components). These regressors and the motion correction parameters were eliminated from the EPI time series. Temporal band-pass filtering (0.01<Hz<0.1) was applied to analyze only rs-fMRI data within this frequency range. The first four rs-fMRI time points were discarded to allow T_1-weighted equilibration of the MRI signal. The mean signal time course within each seed region was employed as "regressor" to assess FC. With the "selxavg3-sess" command line, we performed the first level analysis (single subject analysis) including the computation of the Pearson correlation coefficient (r-value) between the time series within the seed and the time series at each voxel. The obtained correlation maps were then converted

to Z-score maps before entering the second level analysis (group analysis). The "isxconcat-sess" command line was employed to create a "stack" of maps from each subject.

The Desikan-Killiany's Atlas (Desikan et al. 2006) was employed to identify the location of clusters displaying structural MRI differences. Also, two functional atlases focused on cortical (Yeo et al. 2011) and cerebellar (Buckner et al. 2011) networks were used to integrate the information provided by the Desikan-Killiany's Atlas and define the positioning of clusters that show between-group differences or within-group correlations. Mean thickness and z-scores were extracted from each region of interest by employing the "mri_segstats" and "mris_anatomical_stats" command lines.

For each subject, we have performed pair-wise correlations of the time-series obtained, in the right and left hemisphere, in the hippocampus and the entorhinal cortex. Using the Fisher transformation, Pearson's R-values were transformed into a t-values and entered into 1) one sample t-tests to assess whether the connectivity values are significantly greater than zero within each group; 2) ANOVAs to assess between-group differences.

2.6 Statistical analysis

One-way analysis of variance (ANOVA) and Bonferroni post-hoc test were employed to evaluate the group differences regarding demographic/clinical data as well as the hippocampal and entorhinal morphometry. Chi-squared test was used to investigate the group differences on gender and the APOE ε4 carrier status. For analyses related to FC and cortical thickness, general linear models (https://surfer.nmr.mgh.harvard.edu/fswiki/FsgdFormat) were used. The study investigated the differences between groups. The first comparison was HC subjects, nc-MCI patients, c-MCI patients, AD patients; the second comparison HC subjects, MCI^{AD-} subjects, MCI^{AD+} subjects, AD patients; the third comparison HC subjects, nc-MCI^{AD-} subjects, nc-MCI^{AD+} subjects, AD patients. Moreover, further general linear models were used, in the MCI patients, to assess, relationships between FC strength and other variables of interest like the seed morphometric measures, the cortical thickness in each vertex, and CSF biomarkers. The correlation analyses between the variables of interest and the FC of a given seed region FC were performed in a vertex-by-vertex computation by using the "pvr" option in "mri_glmfit" and regressing out the effect of age and educational level. Using the "mri_concat" command line, conjunction maps were created to highlight the sites of overlaps occurring between clusters expressing significant group difference (HC vs. MCI) and clusters that indicate significant correlations between FC strength and variables of interest. To investigate the effect of gender on FC, we took into consideration an additional model with two levels (male and female) and three variables including CSF biomarker levels, age, and educational levels. All the results are shown on statistical maps and adjusted by

applying a cluster-wise correction for multiple comparisons (Hagler et al. 2006). Finally, Spearman's correlation or "mri_glmfit" with --mask (GM of the cerebellum) option was used, respectively, to investigate whether the hippocampal FC with the mPFC or cerebellum was associated with the longitudinal changes in neuropsychological test scores. Longitudinal variations were calculated as the Δ between baseline scores and scores at 24 months. Therefore, MCI subjects with smaller Δ are characterized by better longitudinal preservation of cognitive functions. All statistical tests were two-tailed, and the significant p-value threshold was set at 0.05.

3. Results

3.1 Demographic and clinical features of the study groups

When compared to HC subjects, global cognition and episodic memory (recall and recognition) were affected in MCI subsets and AD groups. AD patients also showed significantly higher frequency of APOE ε4 when compared to nc-MCI or HC subjects. Within the MCI subsets, global cognition and episodic memory (recall) were found to be more compromised in the c-MCI and MCI^{AD+} subsets. Between MCI subsets, no differences were found when considering other neuropsychological and clinical features or the APOE ε4 frequency. AD patients show altered levels of $A\beta_{1-42}$, t-Tau and p-Tau_{181} when compared to HC. No statistically significant differences were found when comparing levels of CSF biomarkers in HC vs. nc-MCI or c-MCI vs. AD. Higher levels of t-Tau, p-Tau_{181}, $A\beta_{1-42}$/t-Tau, and p-Tau_{181}/ $A\beta_{1-42}$ as well as lower $A\beta_{1-42}$ concentrations were found in c-MCI patients when compared to HC subjects and in AD patients compared to nc-MCI or HC subjects. No differences regarding age and educational levels were observed among the study groups (HC, MCI, and AD) or within the MCI subsets (nc-MCI and c-MCI or MCI^{AD-} and MCI^{AD+}). Statistics on demographics and clinical features of the study groups are shown in **Tables 1-3** and **Suppl. Table 1.**

3.2 Morphometric variations in the study groups

Compared to HC or nc-MCI subjects, AD patients showed bilateral hippocampal and entorhinal atrophy. No differences in hippocampal volume or entorhinal thickness were found when comparing AD patients with c-MCI. No statistically significant differences in hippocampal volumes were found in the comparison between the nc-MCI and HC subgroups. However, when compared to HC, c-MCI subjects exhibited signs of atrophy in the right hippocampus and the entorhinal cortex. Entorhinal atrophy in the right hemisphere was also found when comparing c-MCI with nc-MCI subjects. When compared to HC or MCI^{AD-} subjects, MCI^{AD+} exhibited atrophy of the hippocampus. No differences in thickness of the

entorhinal cortex were found when comparing MCI^{AD-} vs. MCI^{AD+} or the two MCI groups with HC. No differences in the estimated total intracranial volume (eTIV) were seen in the study groups. The statistical analysis of the structural data is shown in **Tables 1-2** and **Suppl. Table 1**.

The comparison of AD patients with nc-MCI (**Suppl. Fig. 3A**) or HC (**Suppl. Fig. 3C**) subjects revealed that the AD group shows a greater thinning of brain regions that belong to the Default-Mode Network (DMN) and Posterior Memory Network (PMN). A significant thinning of the mesial temporal areas was instead found in AD patients when compared to c-MCI patients (**Suppl. Fig. 3B**). Finally, no statistically significant differences in cortical thickness were found when comparing c-MCI with nc-MCI patients or HC subjects. A ROI-based analysis confirmed these surface-based results (**Suppl. Table 2)**.

No statistically significant differences in cortical thickness were found when comparing HC vs. MCI^{AD-}, HC vs. MCI^{AD+} or MCI^{AD-} vs. MCI^{AD+}. The comparison of AD patients with MCI^{AD-} (**Suppl. Fig. 4A**) or MCI^{AD+} subjects (**Suppl. Fig. 4B**) revealed that AD individuals show a greater thinning of brain regions that belong to the DMN/PMN and the salience Network (SN)/Cingolo-Opercular Network (CON). These changes were more patent in the AD vs. MCI^{AD-} comparison. Compared to MCI^{AD-} subjects, AD patients displayed signs of atrophy in the medial prefrontal cortex (mPFC) and the superior parietal gyrus.

3.3 Hippocampal FC variations in subsets of MCI subjects

The analysis of the hippocampal FC of MCI subgroups identified the presence of significant differences. First, we evaluated nc-MCI and c-MCI subjects. Compared to HC subjects, nc-MCI patients showed enhanced FC between the hippocampus and the mPFC as well as the cerebellar regions that are part of DMN, the thalamus, and the striatum. The analysis also indicated reduced FC between the hippocampus and the brainstem (**Fig. 1A**). c-MCI patients showed hypo-connectivity of the hippocampus with the thalamus or the cerebellar areas that are part of the DMN and dorsal attentional network (DAN) and no differences in hippocampal FC with the rest of the cortex (**Fig. 1B**). Finally, the direct comparison within the nc/c MCI subset revealed that nc-MCI patients show hyper-connectivity between the hippocampus and the cerebellar areas that are functionally associated with the DMN, the Salience Network (SN)/Cingolo-Opercular Network (CON) as well as the limbic system (**Fig. 1C**). Compared to nc-MCI subjects, AD patients showed diffuse patterns of hypo-connectivity between the hippocampus and cortical and cerebellar regions that are mainly involved in the DMN/PMN, the thalamus, or the brainstem. The hippocampus was also hypo-connected with the insula and sensorimotor regions as well as with cerebellar areas that are part of the limbic system (**Fig. 2A**). No significant differences were found by comparing c-MCI and AD groups. When compared to HC subjects,

AD patients showed decreased FC between the hippocampus and cortical and cerebellar regions that are part of the DMN/PMN, the striatum, and the brainstem. Moreover, hypo-connectivity of the hippocampus was observed with cerebellar regions of sensorimotor networks (**Fig. 2B**).

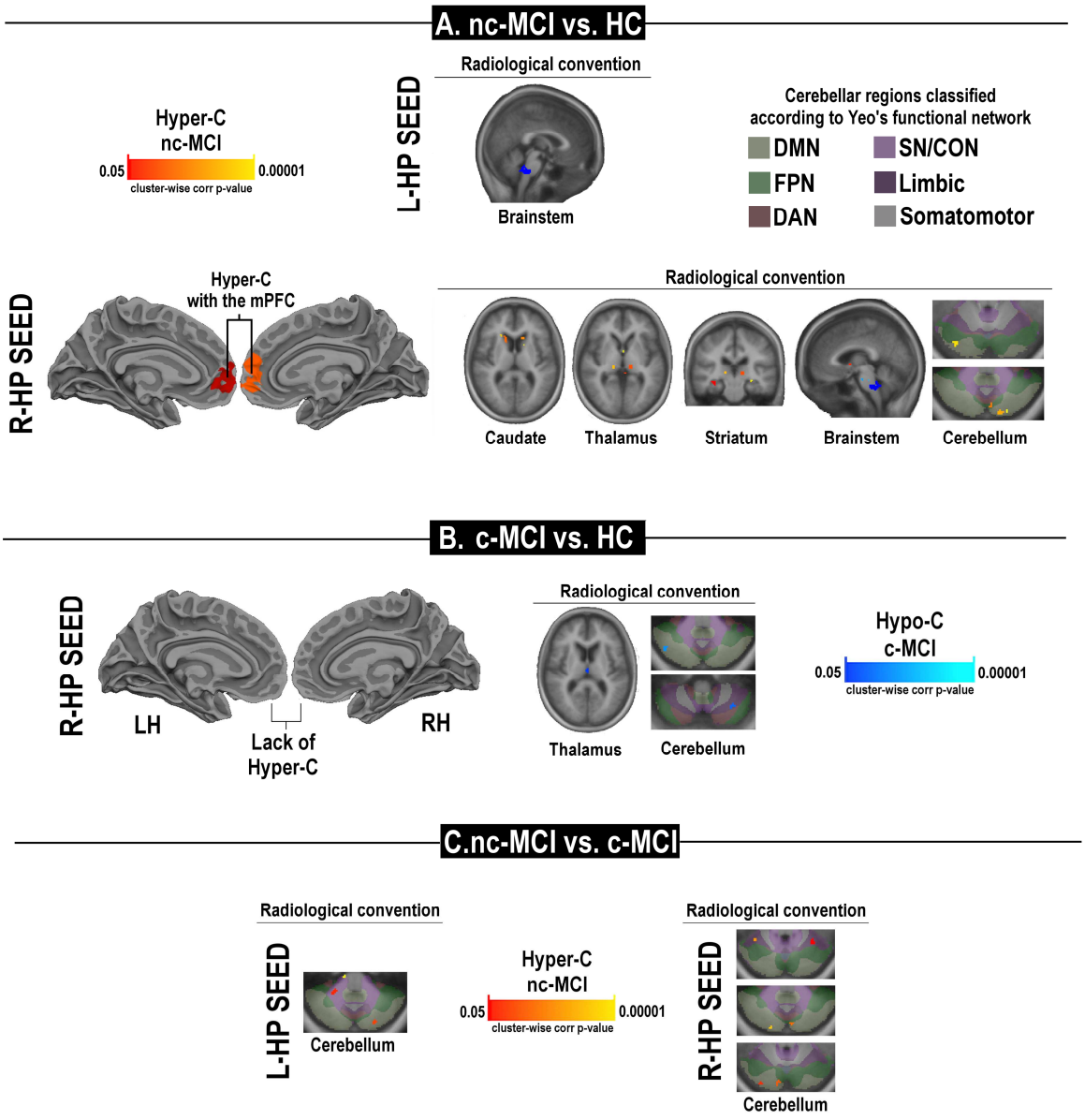

Figure 1. Statistical maps of differences in hippocampal (HP) functional connectivity of MCI subsets. Panel A shows the comparison between nc-MCI and HC subjects; panels B and C show the comparison of c-MCI subjects with HC or nc-MCI subjects, respectively. The figure depicts areas with a cluster-wise probability below the corrected p-value of 0.05. Pseudocolor scales indicate the statistical strength of the hyper-connectivity (Hyper-C) or hypo-connectivity (Hypo-C). Clusters changing from red to yellow or from dark blue to light blue indicate increased hyper-C or hypo-C, respectively. *Abbreviations:* DAN=Dorsal Attention Network; DMN=default-mode network; FPN=fronto-parietal network;

SN/CON=Salience/Cingulo-Opercular Networks; L=left; LH=left hemisphere; mPFC=medial prefrontal cortex; R=right; RH=right hemisphere.

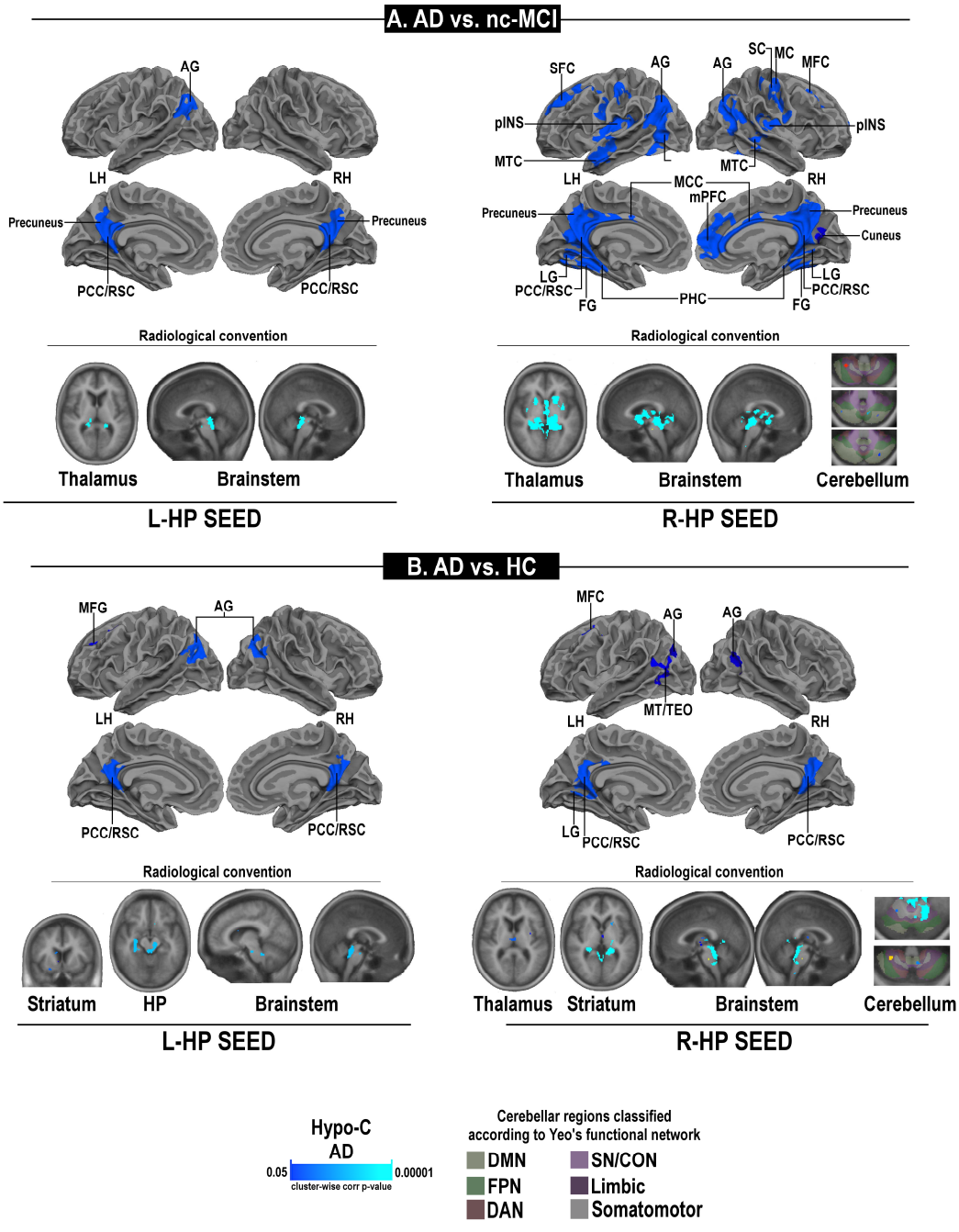

Figure 2. Statistical maps of differences in hippocampal (HP) functional connectivity of AD patients. Significant hypo-connectivity is observed in AD patients when compared to nc-MCI (panel A) or HC subjects (panel B). The figure depicts areas with a cluster-wise probability below the corrected p-value

of 0.05. Pseudocolor scales, with clusters changing from dark blue to light blue, indicate the statistical strength of the hypo-connectivity (Hypo-C).
Abbreviations: AG=angular gyrus; DAN=Dorsal Attention Network; DMN=default-mode network; FG=fusiform gyrus; FPN=fronto-parietal network; IPL=interior parietal lobe; L=left; LH=left hemisphere; LG=lingual gyrus; MC=motor cortex; MCC=middle cingulate cortex; MFG/MFC=middle frontal gyrus/cortex; MTC= middle temporal cortex; pINS=posterior insula; SMA=supplementary motor area; mPFC=medial prefrontal cortex; PCC/RSC=posterior cingulate cortex/retrosplenial cortex; PHC=parahippocampal cortex; R=right; RH=right hemisphere; SC=sensory cortex; SFC =superior frontal cortex; SN/CON=Salience/Cingulo-Operacular Networks.

We also analyzed MCI subjects taking into account their load of AD-related pathology as expressed by altered values of an AD-related biomarker, the p-Tau_{181}/ $A\beta_{1-42}$ ratio. Compared to HC subjects, MCI^{AD-} individuals exhibited hippocampal hyper-connectivity with the mPFC, the cortical and cerebellar regions that are part of the DMN, the amygdala, the hypothalamus, the striatum, and the thalamus (**Fig. 3A**). On the other hand, MCI^{AD+} individuals showed no differences in hippocampal FC with the cortex, but hypo-connectivity with cerebellar regions that are part of the DMN. We also found mixed patterns of hypo-/hyper-connectivity with cerebellar regions that are part of the FPN as well as hyper-connectivity with cerebellar regions that are functionally linked to the limbic system (**Fig. 3B**). The MCI^{AD-} vs. MCI^{AD+} comparison revealed that MCI^{AD-} subjects show hippocampal hyper-connectivity with cortical and cerebellar regions that participate in the DMN as well as with the amygdala, the striatum, and the thalamus (**Fig. 3C**). Compared to MCI^{AD-} subjects, AD patients showed diffuse patterns of hippocampal hypo-connectivity with DMN/PMN- and SN- related cortical areas as well as with the brainstem, the hypothalamus, the thalamus, the limbic system, and the striatum (**Fig. 3D**). On the other hand, compared MCI^{AD+} subjects, AD patients showed hippocampal hypo-connectivity with core regions of the DMN/PMN and SN (posterior insula) as well as with the hypothalamus, the thalamus, the limbic system and the striatum (**Fig. 3E**).

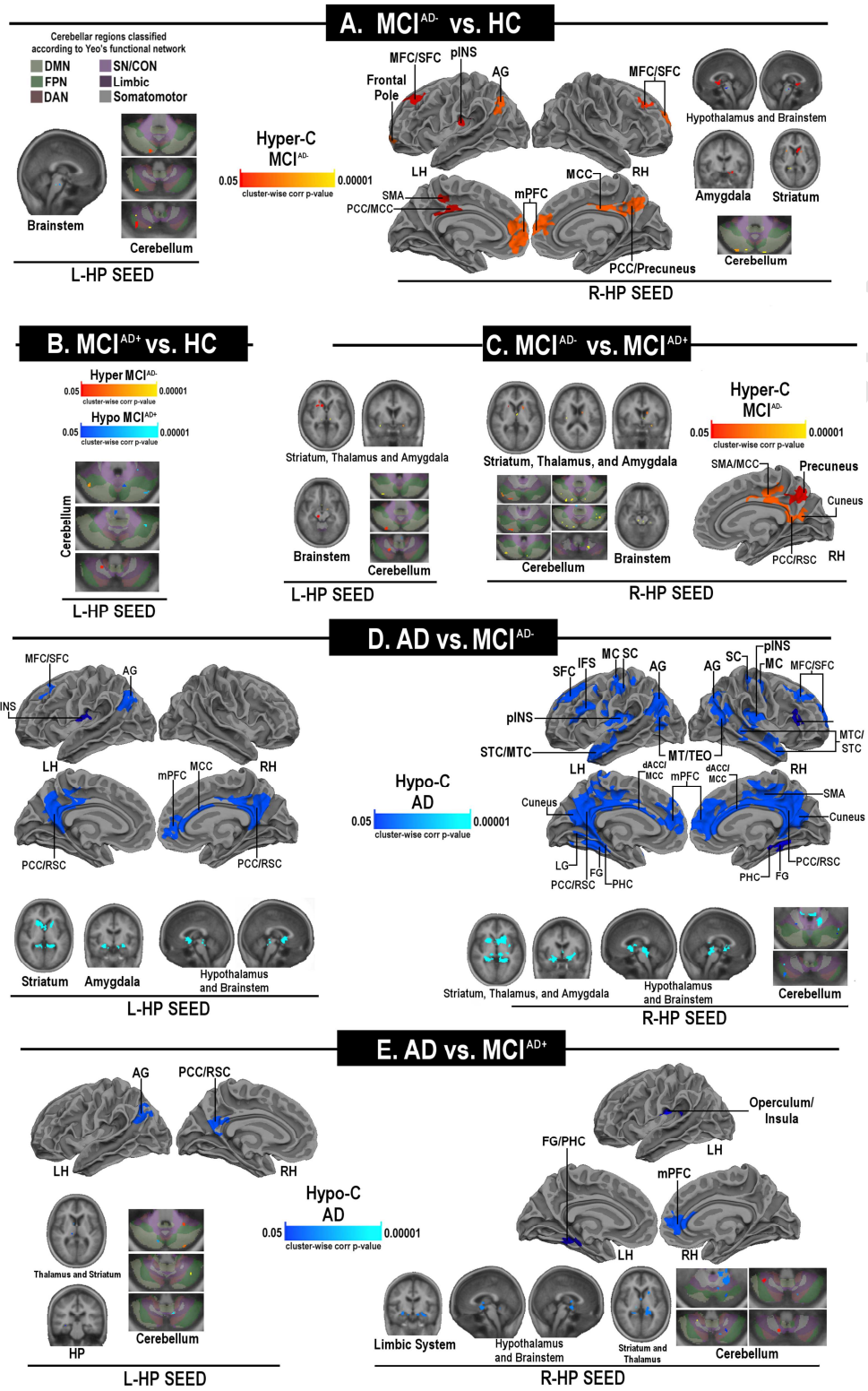

Figure 3. Statistical maps of differences in hippocampal (HP) functional connectivity of MCI subtypes categorized by the p-Tau/Aβ ratio. Panels A and B show the comparison between HC and MCI^{AD-} or MCI^{AD+} individuals, respectively; panels C show the comparison between the two MCI subsets. Panel D

and E show connectivity changes in AD patients when compared to MCI^{AD-} or MCI^{AD+} subjects, respectively. The figure depicts areas with a cluster-wise probability below the corrected p-value of 0.05. Clusters changing from red to yellow or from dark blue to light blue indicate increased hyper-C or hypo-C, respectively.
Abbreviations: AG=angular gyrus; dACC= dorsal Anterior Cingulate Cortex; DAN=Dorsal Attention Network; DMN=default-mode network; FG=fusiform gyrus; FPN=fronto-parietal network; L=left; LH=left hemisphere; LG=lingual gyrus; IFS=inferior frontal sulcus; MC=motor cortex; MCC=middle cingulate cortex; MFG/MFC=middle frontal gyrus/cortex; MTC= middle temporal cortex; SMA=supplementary motor area; mPFC=medial prefrontal cortex; PCC/RSC=posterior cingulate cortex/retrosplenial cortex; PHC=parahippocampal cortex; pINS=posterior insula; R=right; RH=right hemisphere; SC=sensory cortex; SFC =superior frontal cortex; SN/CON=Salience/Cingulo-Operacular Networks; STC=superior temporal cortex.

Finally, we assessed the FC changes in the nc-MCI set taking into account their load of AD-related pathology. Compared to HC subjects, nc-MCI^{AD-} individuals showed hippocampal hyper-connectivity with regions of the DMN and the cerebellum (**Suppl. Fig. 5A**). On the other hand, when compared to HC subjects, nc-MCI^{AD+} did not display hippocampal hyper-connectivity with DMN-related areas but showed the presence of small-size clusters of mixed patterns of hyper-connectivity and hypo-connectivity occurring between the hippocampus and the cerebellum. This set also showed hypo-connectivity of the hippocampus with the amygdala and the striatum (**Suppl. Fig. 5B**). Compared to nc-MCI^{AD+}, nc-MCI^{AD-} individuals, showed hyper-connectivity with the cerebellum and the striatum (**Suppl. Fig. 5C**).

3.5 Entorhinal cortex FC variations in subsets of MCI subjects

As with the hippocampus we first analyzed MCI patients categorized by their clinical follow-up. Compared to HC, nc-MCI patients showed hyper-connectivity with cerebellar areas that are part of the DMN, the FPN, the SN/CON and the limbic system (**Fig. 4A**). Conversely, compared to HC (**Fig. 4B**) or nc-MCI subjects (**Fig. 4C**), c-MCI patients showed reduced connectivity with the lateral-occipital cortex, the cortical and cerebellar regions that are part of the FPN and DAN, the cerebellar regions of the Salience/Cingulo-Opercular Networks (SN/CON) and the limbic system as well as the brainstem, the striatum, and the thalamus. Compared to nc-MCI subjects, AD patients showed diffuse patterns of entorhinal hypo-connectivity with the cerebellum, the cortical regions that are mainly involved in the SN/CON and VAN as well as the thalamus, the striatum and the brainstem (**Fig. 5A**)**.** In contrast, compared to c-MCI individuals, AD patients did not show differences in hippocampal or entorhinal FC. When compared to HC subjects**,** AD patients displayed hypo-connectivity of the entorhinal cortex with

regions of the SN/CON, the cerebellum, the brainstem, the thalamus, the striatum, and the limbic system (**Fig. 5B**).

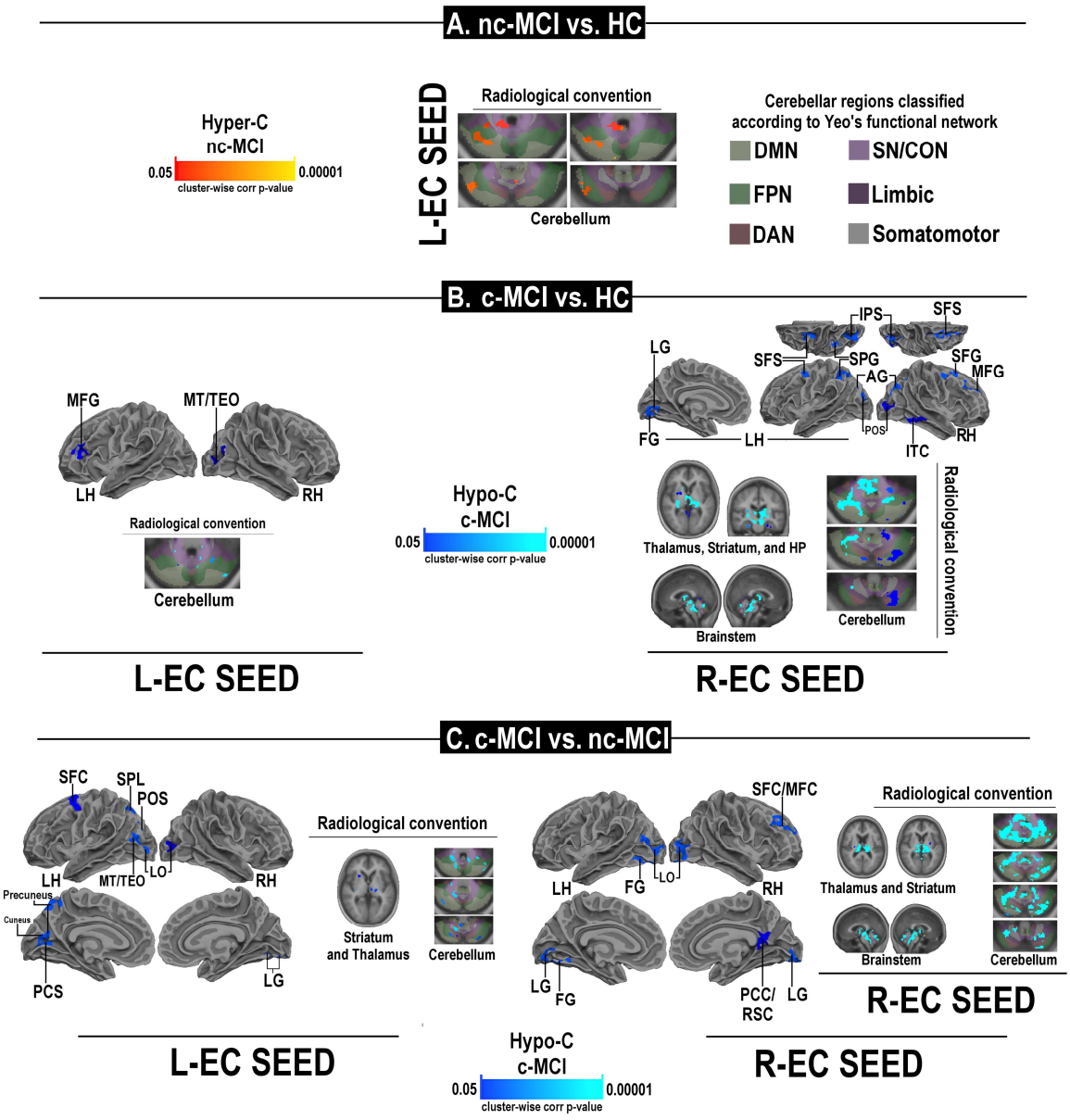

Figure 4. Statistical maps of differences in entorhinal (EC) functional connectivity of MCI subsets. Panel A shows the comparison between nc-MCI and HC subjects; panels B and C show the comparison of c-MCI subjects with HC or nc-MCI subjects, respectively. The figure depicts areas with a cluster-wise probability below the corrected p-value of 0.05. Clusters changing from red to yellow or from dark blue to light blue indicate increased hyper-C or hypo-C, respectively.
Abbreviations: AG=angular gyrus; DAN=Dorsal Attention Network; DMN=default-mode network; FG=fusiform gyrus; FPN=fronto-parietal network; IPS=intraparietal sulcus; ITC=inferior temporal cortex; L=left; LG=lingual gyrus; LH=left hemisphere; LO=lateral-occipital; MFC= middle frontal cortex;

MFG=middle frontal gyrus; PCC/RSC=posterior cingulate cortex/retrosplenial cortex; PCS=paracingulate sulcus; POS=parieto-occipital sulcus; R=right; RH=right hemisphere; SN/CON=Salience/Cingulo-Operacular Networks; SFC =superior frontal cortex; SFG=superior frontal gyrus; SFS=superior frontal sulcus; SPG=superior parietal gyrus; SPL=superior parietal lobe.

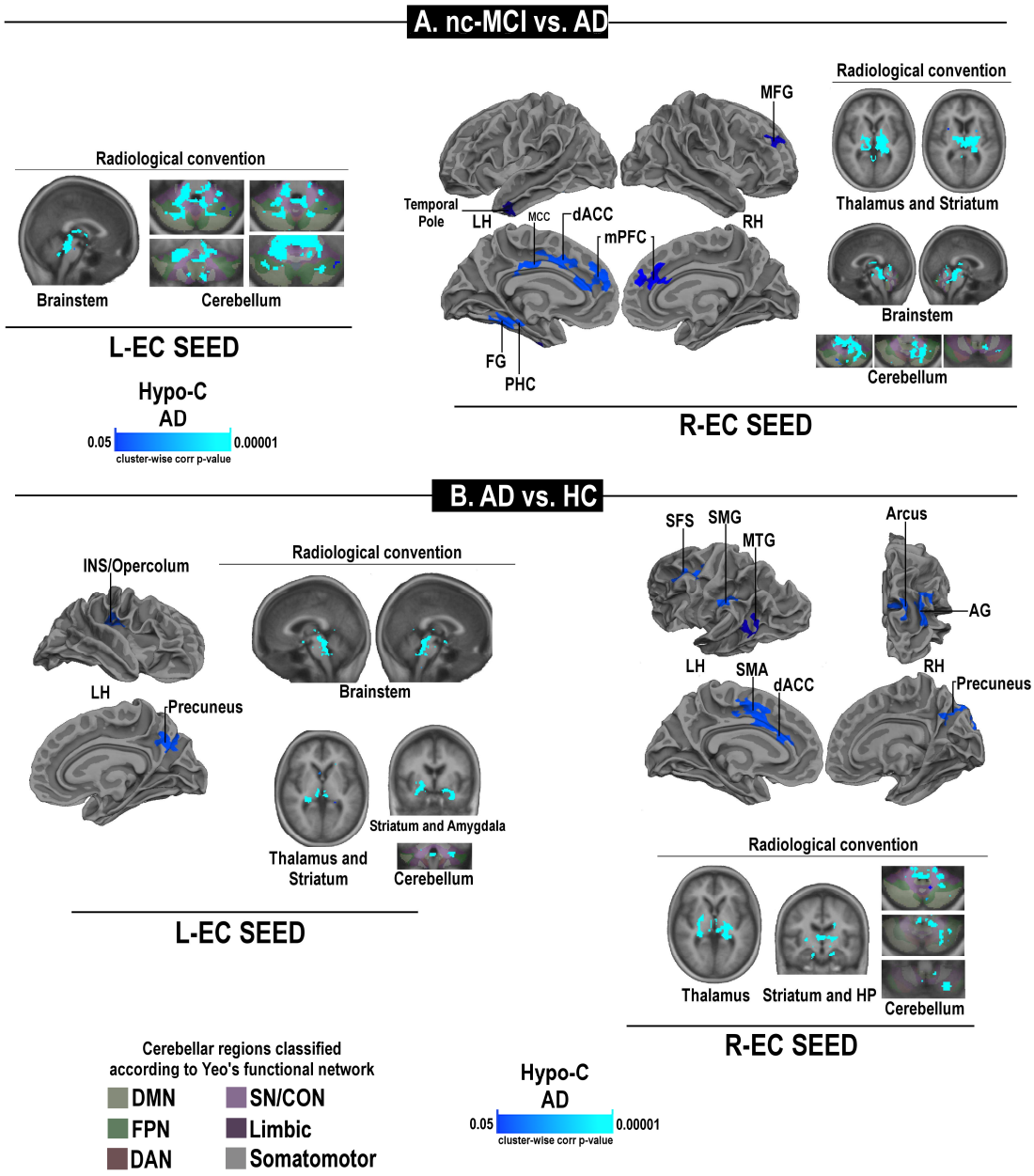

Figure 5. Statistical maps of differences in entorhinal (EC) functional connectivity of AD patients. Significant hypo-connectivity is observed in AD patients when compared to nc-MCI (panel A), c-MCI (panel B), or HC subjects (panel C). The figure depicts areas with a cluster-wise probability below the corrected p-value of 0.05. Pseudocolor scales, with clusters changing from dark blue to light blue, indicate the statistical strength of the hypo-connectivity (Hypo-C).

Abbreviations: AG=angular gyrus; dACC=dorsal anterior cingulate cortex; DAN=Dorsal Attention Network; DMN=default-mode network; FG=fusiform gyrus; FPN=fronto-parietal network; INS=insula; L=left; LH=left hemisphere; MCC=middle cingulate cortex; MFC=middle frontal cortex; mPFC=medial prefrontal cortex; MTG=middle temporal gyrus; PHC=parahippocampal cortex; R=right; RH=right hemisphere; SFS =superior frontal sulcus; SMG= supramarginal gyrus; SMA=Supplementary Motor Area; SN/CON=Salience/Cingulo-Operacular Networks.

In the second analysis, we evaluated the MCI subjects subdivided by their loads of AD-related pathology. In this second set, we found, that compared to HC subjects, MCI^{AD-} individuals showed hyper-connectivity of the entorhinal cortex with the cerebellar regions that are part of the DMN and sensorimotor network as well as with the brainstem and the striatum (**Fig. 6A**). In contrast, MCI^{AD+} showed hypo-connectivity with the lateral-occipital area, the striatum, and the limbic system as well as hyper-connectivity with the hypothalamus. We also found a mixed pattern of hyper- and hypo-connectivity occurring between the entorhinal cortex and selected cerebellar regions (**Fig. 6B**). The direct comparison between the two MCI subsets revealed that MCI^{AD+} subjects show entorhinal hypo-connectivity with the sensorimotor cortex, associative motor areas, DMN-related cerebellar areas as well as the hypothalamus and the brainstem (**Fig. 6C**). Compared to MCI^{AD-} subjects, AD patients showed patterns of hippocampal hypo-connectivity with the cerebellum, SN-related cortical areas, and the sensorimotor network as well as the brainstem, the hypothalamus, the limbic system, the striatum, and the thalamus (**Fig. 6D**). Compared to MCI^{AD+} individuals, AD patients showed hippocampal hypo-connectivity with FPN- and SN-related cerebellar areas, the sensorimotor network, the brainstem, the striatum, and thalamus (**Fig. 6E**).

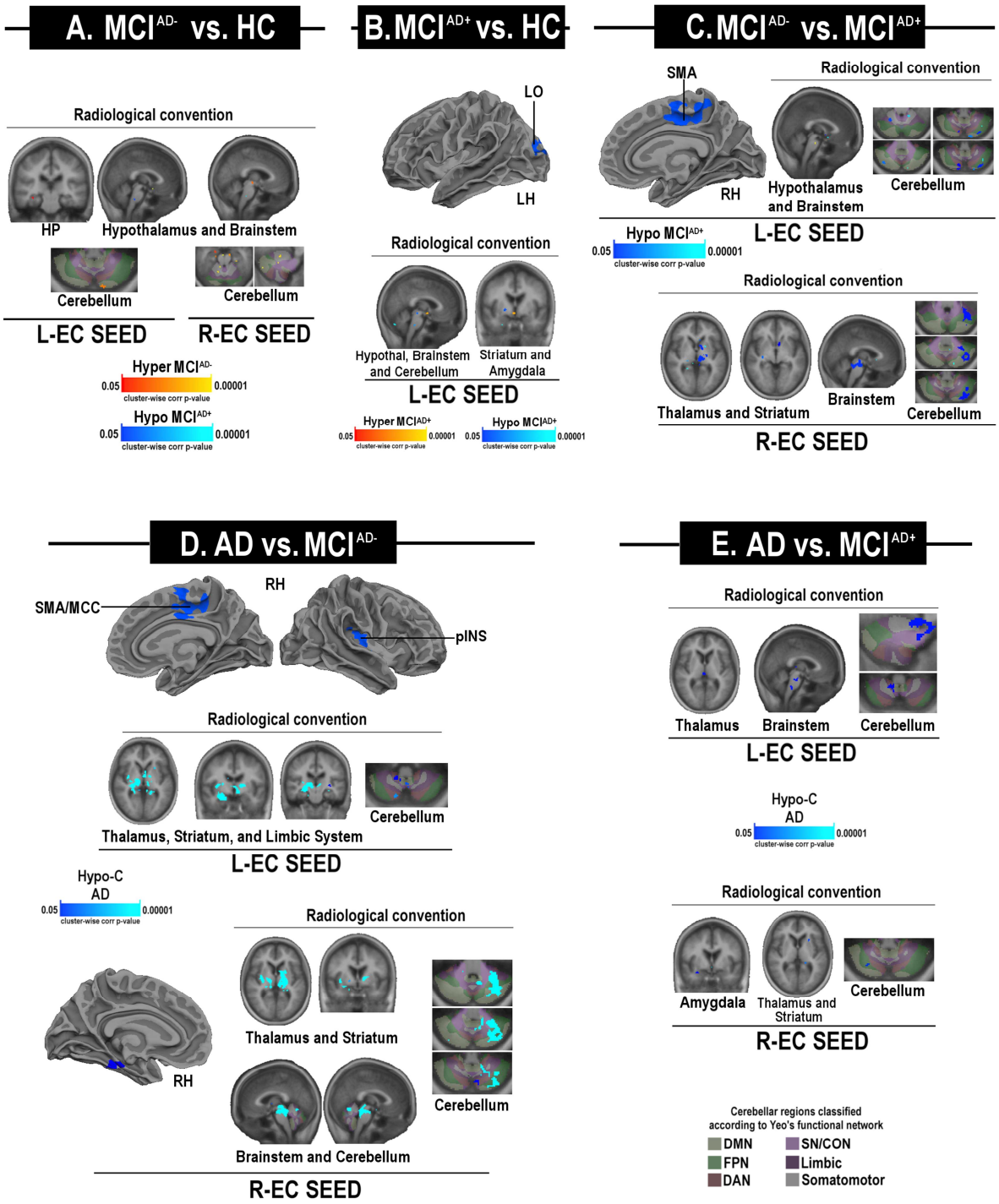

Figure 6. Statistical maps of differences in entorhinal (EC) functional connectivity of MCI subtypes categorized by the p-Tau/Aβ ratio. Panels A and B show the comparison between HC and MCI^{AD-} or MCI^{AD+} individuals, respectively; panels C show the comparison between the two MCI subsets. Panel D and E show the connectivity changes in AD patients when compared to MCI^{AD-} or MCI^{AD+} subjects, respectively. The figure depicts areas with a cluster-wise probability below the corrected p-value of 0.05.

Clusters changing from red to yellow or from dark blue to light blue indicate increased hyper-C or hypo-C, respectively.
Abbreviations: DAN=Dorsal Attention Network; DMN=default-mode network; FPN=fronto-parietal network; L=left; LH=left hemisphere; LO=lateral-occipital; MCC=middle cingulate cortex; pINS=posterior insula; SMA=supplementary motor area; R=right; RH=right hemisphere; SN/CON=Salience/Cingulo-Operacular Networks.

The third analysis investigated the nc-MCI group in reference to different loads of AD-related pathology. We found that, compared to HC (**Suppl. Fig. 6A**) or nc-MCI^{AD+} (**Suppl. Fig. 6C**), nc-MCI^{AD-} subjects showed hippocampal hyper-connectivity with selected cerebellar regions. In contrast, when compared to HC subjects, nc-MCI^{AD+} subjects displayed small clusters of hyper-connectivity between the entorhinal cortex and selected subcortical areas (**Suppl. Fig. 6B**).

3.7 Relationship of rs-fMRI data with age, morphometry, CSF biomarkers and longitudinal changes in cognition

In the MCI group, using a whole brain correlation analysis, we found that the features of hippocampal FC were associated with altered CSF levels of p-Tau and amyloid. Increased FC, occurring between the hippocampus and DMN regions, was negatively associated with levels of p-Tau$_{181}$ and p-Tau$_{181}$/Aβ_{1-42}, and positively associated with Aβ_{1-42} levels (**Suppl. Fig. 7**). The strength of the hippocampal FC did not correlate with age, educational level or alterations in the structural integrity of the hippocampus or cortex. No significant effect was found as far as the synergistic interaction of gender with respect to CSF AD-related biomarkers. In the entorhinal cortex, the strength of FC positively correlates with the structural integrity of the seed (**Suppl. Fig. 8**). Finally, increased hippocampal FC with the mPFC was significantly and positively associated with a smaller longitudinal decline in the Boston Naming Test (BNT) and the Trail Making Test-A (TMTA) tests, two tests that evaluate naming and executive functions. The parameter also showed a trend towards significance when considering the correlation with longitudinal changes in scores of the AVDEL30 (**Table 3-4**). Moreover, the increase of hippocampal FC was significantly associated with smaller longitudinal variations in cognition. Conjunction maps show that these relationships are linked to variations of episodic memory (RAVLT) and executive functions (TMTB) (**Fig. 7**). These findings indicate that the increased hippocampal FC can help to maintain performances in subsets of cognitive domains.

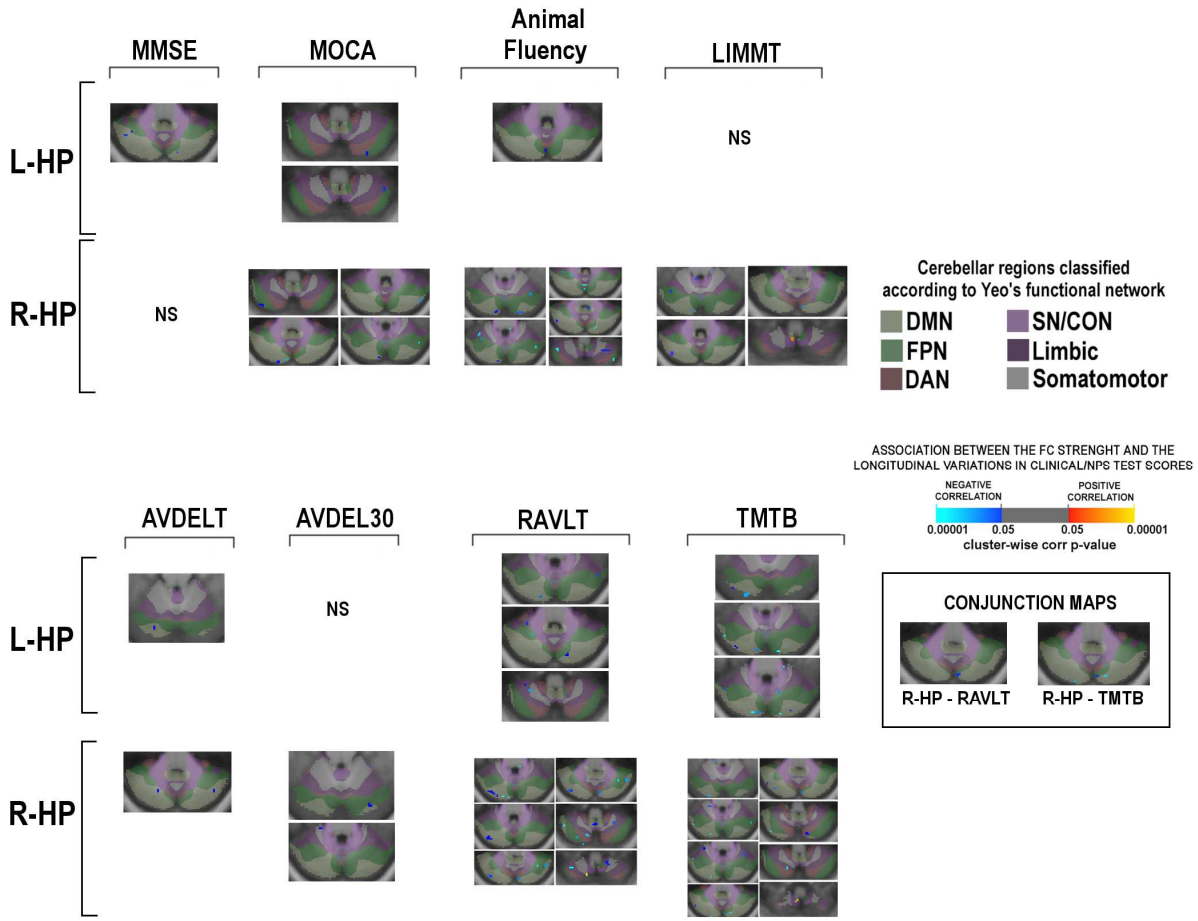

Figure 7. Whole-cerebellum correlation analysis between hippocampal (HP) functional connectivity and longitudinal variations of neuropsychological/clinical scores. Each conjunction map shows the intersection of significant clusters that indicate correlations between FC and longitudinal variations of RAVLT and TMTB scores and clusters expressing significant FC differences in the comparisons between nc-MCI and c-MCI. Clusters changing from red to yellow or from dark blue to light blue indicate positive or negative correlations, respectively. Images are shown in radiological convention. Note that the enhanced hippocampal FC is associated with lower longitudinal decline in cognitive domains assessed by the RAVLT and TMTB tests.
Abbreviations: BNT=Boston Naming Test; AVDELT= Rey Auditory Verbal Learning Test-Delayed Recognition Score; AVDEL30=Rey Auditory Verbal Learning Test-Delayed 30 Minute Delay Total; LDEL= LIMMT=Logical Memory-Immediate Recall Total Number of Story Units Recalled; NS=not significant; TMTB=Trail Making Test Part B; RAVLT=Rey Auditory Verbal Learning Test Immediate.

4. Discussion

In the present study, we investigated patterns of hippocampal and entorhinal FC in a cohort of HC, MCI and AD subjects. The rs-fMRI data were also evaluated in relation to the clinical progression

and degrees of AD-pathology of MCI subjects. Overall, the analysis indicates that AD patients show a parallel process of hypo-connectivity that is localized in the hippocampus and entorhinal cortex. The analysis of the MCI subsets shows that c-MCI and MCI^{AD+} subjects are characterized by hypo-connectivity of the entorhinal cortex and hippocampus while nc-MCI, and MCI^{AD-} subjects exhibit hyper-connectivity of the two regions.

4.1 Patterns of functional connectivity, cognitive status and structural damage of AD patients

Our AD subjects were characterized by the collapse of hippocampal and entorhinal connectivity, the decline in memory and executive skills, and the presence of marked signs of cortical and subcortical atrophy. These findings confirm the notion that macro-structural damage severely impairs global communication efficiency, prevents the adaptive functional reorganization of the brain networks, ultimately setting the stage for the disease progression (Hillary and Grafman 2017). Of note, we observed hypo-connectivity in the angular gyrus and retrosplenial/posterior cingulate cortex, two areas that are strictly involved in memory retrieval and intimately connected to the hippocampus and entorhinal cortex (Eichenbaum 2017; Sestieri et al. 2017). It is therefore conceivable that, in AD subjects, the reduced connectivity of the hippocampus and entorhinal cortex represents a functional correlate of the defective episodic memory retrieval that is found in the disease.

4.2 Patterns of functional connectivity, cognitive status, and structural features of nc-MCI and MCI^{AD-} subjects

Our study shows that nc-MCI and MCI^{AD-} individuals exhibit hippocampal and entorhinal hyper-connectivity as well as the relative preservation of cognitive functions and brain structures.

The hippocampal hyperactivity exhibited by MCI patients is controversial in value. While some authors have proposed that the process plays a compensatory role and helps to maintain cognitive performances (Bondi et al. 2005; Dai et al. 2009; Dickerson et al. 2008; Kircher et al. 2007; Oh and Jagust, 2013; Huijbers et al. 2015; Mormino et al. 2011; Putcha et al. 2011; Schultz et al. 2017; Sperling et al. 2009), others have considered the phenomenon disadvantageous and set to promote cognitive impairment (Das et al. 2013; Pasquini et al. 2015).

Furthermore, previous studies have indicated that MCI patients show hyper-connectivity or hyper-activity that is regionally restricted within the medial temporal lobe (MTL) while reduced connectivity occurs between MTL and other network nodes, including the DMN. These intra-MTL effects have been confirmed by Arterial Spin Labeling studies (Alsop et al. 2008; Alsop et al. 2010), task fMRI (Yassa et al. 2010b), and rs- fMRI (Das et al. 2013; Pasquini et al. 2015). We have performed the

MTL analysis and found that, compared to HC or nc-MCI groups, the mean values of intra-MTL connectivity are higher in the AD or c-MCI sets. However, these FC differences did not reach statistical significance (data not shown), thereby suggesting differences between our and the other (Das et al. 2013; Pasquini et al. 2015) datasets.

Our results, indicating the presence of enhanced FC between the hippocampus, thalamus, striatum, and the mPFC support the "compensatory hypothesis" for the hyperconnectivity that we have detected. The thalamus is a structural and functional hub for the communication occurring between the hippocampus and mPFC, thereby favoring strategic cognitive functions, including memory consolidation (Ferraris et al. 2018; Eichenbaum 2017). The striatum, along with the PFC, is also implicated in the modulation of memory retrieval (Scimeca and Badre 2012). The mPFC is part of an integrated system, the DMN, that sustains the global communication and meta-stability of the brain (Hellyer et al. 2014) and, ultimately, affects a wide-range of high-order cognitive functions as well as the resilience against neurodegenerative processes (Hillary and Grafman 2017). The hippocampal hyper-connectivity with the mPFC is in line with different proposed modelizations of brain ageing (i.e., HERA, HAROLD, PASA, CRUNCH, STAC, GOLDEN Aging) that postulate that the increased engagement of the prefrontal brain regions is set to compensate the functional decline occurring in posterior regions of the brain(Tulving et al. 1994; Cabeza et al. 1997; Davis et al. 2008; Schneider-Garces et al. 2010; Park and Reuter-Lorenz 2009; Reuter-Lorenz and Park 2014; Fabiani 2012). The compensatory hypothesis fits with evidence indicating that the mPFC and the hippocampus are tightly interconnected by bidirectional projections that are structurally and functionally integrated. The oscillatory synchronic activity between these two regions supports the organization and processing of the episodic memory (Eichenbaum 2017). The mPFC is strategic for memory as the area receives information on contextual cues from the anterior hippocampus and, in turns, indirectly sends the information - via the thalamus and perirhinal/entorhinal cortices- to the posterior hippocampus (**Suppl. Fig. 9**). In this context, the hippocampus acts as a key region that is set to control memory organization and encoding whereas the mPFC is implicated in the retrieval of context-appropriate memory engrams, the suppression of distractors or the interference and switching or selection of episodic memories according to contextual rules (Eichenbaum 2017). Furthermore, the presence of altered connectivity between the mPFC and the hippocampus impairs the object-place and temporal-order memory and leads to severe impairment of conditional visual discrimination as well as to learning and memory deficits related to defective suppression of irrelevant memory engrams (Eichenbaum 2017; Barker et al. 2007). In summary, the enhanced FC between the

hippocampus and the mPFC that we observed in the nc-MCI group is likely to result in positive cognitive outputs.

Our findings also unravel a functional connection between the hippocampus and the cerebellum. The comparison with HC subjects or within MCI subsets revealed that nc-MCI and MCI^{AD-} individuals show hippocampal hyper-connectivity with cerebellar areas that are functionally associated with the DMN. The interplay between these regions - through circuits that involve the entorhinal cortex, the cerebellum-thalamo-cortical, and cortical-ponto-cerebellar pathways - is strategic for the modulation of cognitively-relevant prefrontal and parietal activities (Yu and Krook-Magnuson 2015). The involvement of the cerebellum is intriguing as recent evidence indicate that the region acts as a critical hub for the control of a wide range of cognitive processes encompassing language, visual-spatial, executive, and working memory processes (Stoodley 2012). In that regard, we found that the hippocampal hyper-connectivity of the nc- or MCI^{AD-} subsets was associated with the preservation of cognition, and mnestic and executive functions, in particular, thereby suggesting that the cerebellum can be strategically involved in maintaining the cognitive reserve (**Fig.7**)**.**

From a theoretical standpoint, the increased FC that we observed in nc-MCI subjects may help to cope with and counteract, the undergoing neurodegenerative process and related cognitive impairment. These speculative considerations are inferred from a model that is pseudo-longitudinal as the dataset offers information on the clinical progression but not on the related longitudinal FC changes. However, the overlap of findings that we observed between nc-MCI subjects who are also MCI^{AD-} lend support to the idea that the hippocampal hyper-connectivity of MCI individuals - when the AD-related pathology is not present or at sub-threshold levels - serves as a valuable adaptive strategy to maintain cognitive functions. Our findings also lend support to the possibility of a previously described "inverse-U-shaped" model and proposes that divergent patterns of hippocampal FC can be used as functional biomarker to identify the presence or absence of dynamic processes that drive MCI subjects to AD (Dickerson and Sperling, 2008; Sperling et al. 2010; Sperling et al. 2014; Schultz et al. 2018).

4.3 Patterns of functional connectivity, cognitive status and structural alterations in c-MCI and MCI^{AD+} subjects

c-MCI and MCI^{AD+} subjects did not show signs of hippocampal hyper-connectivity with the mPFC, DMN-related areas or the cerebellum. This lack of hyper-connectivity may result in reduced compensatory engagement of critical regions that are involved in the brain meta-stability and lead to more severe cognitive decline. c-MCI and MCI^{AD+} individuals also showed entorhinal hypo-connectivity with cortical and cerebellar regions that take part in the modulation of long-term memory and

attentional systems. The entorhinal hypo-connectivity should be considered in relation to the role played by the superficial layers, II-III, of this region (**Suppl. Fig. 9**). These layers act as relay stations that carry, through the perirhinal or parahippocampal cortices, unimodal/multimodal cortical information from cortical associative areas to the hippocampus (Canto et al. 2008; Ranganath and Ritchey 2012). Moreover, the deep layers, V-VI, of the lateral entorhinal cortex send projections from the posterior hippocampus, via the cingulum, to the parahippocampus and the cortical areas that are involved in attentional networks and the DMN/PMN bundle (Kahn et al. 2008; Lacy and Stark 2012; Libby et al. 2012). These circuits promote the integration of spatial information as well as the representation of retrieved events (Preston and Eichenbaum 2013; Vann et al. 2009). It is therefore conceivable that, in c-MCI subjects, reduced FC with the DMN and associative networks represents a functional marker of underlying alterations that occur before the onset and development of AD.

In line with previous MRI studies (Dickerson et al. 2001; Grundman et al. 2002; Jack et al. 2004; Apostolova et al. 2006; Henneman et al. 2009), c-MCI patients show mesial temporal atrophy in the hippocampus and entorhinal cortex. Although some studies have reported the presence of cortical atrophy in MCI subjects (Tabatabaei-Jafari et al. 2015), our MCI individuals were characterized by relative preservation of the cortical thickness. In that regard, it should be underlined that these patients did not show a substantial impairment of the global cognitive functions. In addition, our study subjects were highly educated individuals who likely possessed significant levels of cognitive reserve (Lo and Jagust 2013).

Overall, these data are in agreement with neuropathological evidence indicating that the entorhinal cortex and the hippocampus are the first brain regions to display tau-pathology and neurodegeneration in the course of AD (Braak et al. 1994). In line with this notion, our c-MCI patients showed decreased CSF levels of $A\beta_{1-42}$ and increased levels of t-Tau, p-Tau_{181}, t-Tau/$A\beta_{1-42}$, and p-Tau_{181}/$A\beta_{1-42}$, alterations that went along with the presence of more significant memory deficits.

The correlation between altered CSF features and the presence of mPFC-related modifications is in accordance with studies showing that decreased FC between central hubs of the DMN correlates with enhanced Aβ deposition (Buckner RL et al. 2005; Elman et al. 2016; Foster et al. 2018; Grothe et al. 2016; Koch et al. 2010; Mutlu et al. 2017; Mormino et al. 2011; Palmqvist et al. 2017). fMRI/PET studies have recently shown that increased levels of tau-related pathology lead to a progressive decline of the brain FC (Cope et al. 2018; Hoenig et al. 2018; Jones et al. 2016; Sepulcre et al. 2017) and reduced activation of the DMN in particular (Hoenig et al. 2018). Schultz and colleagues (2017) have also suggested that, upon pre-symptomatic AD, a transient hyper-connectivity phase is followed by hypo-

connectivity. The authors reported that DMN connectivity is negatively associated with global cortical deposition of amyloid and the presence of PET-related signs of tau pathology in the MTL and inferior parietal cortices. These fMRI/PET findings and our data fit with a model in which the appearance of signs of tau-pathology go along with the loss of hippocampal GABAergic interneurons that may be instrumental in setting the stage for regional hyperexcitability (Levenga et al. 2013).

We, therefore, propose a "work in progress" model (**Fig. 8**) where patterns of altered hippocampal FC can serve as a proxy functional biomarker of the susceptibility to AD status of subsets of MCI subjects. The model proposes a two-stage process. In MCI^{AD-} patients, the benign, para-physiological, occurrence of tau deposition that is restricted to the MTL (Braak and Braak 1994; Braak et al. 2013) (Scholl et al. 2016; Ossenkoppele et al. 2016) may favor a down-regulation of GABAergic neurotransmission that sustains a compensatory and cognitively-relevant enhanced glutamatergic neurotransmission and excitability. In MCI^{AD+} patients, the pathological load produced by the convergence of amyloid-dependent and -independent mechanisms may accelerate injurious tau deposition outside of the MTL (Braak and Braak 1994; Braak et al. 2013), unleash a glutamatergic overdrive, and favors the onset of pathological hyperexcitability, excitotoxicity, micro/macro-structural damage, atrophy, deficient hippocampal functioning, and the progression of cognitive and behavioral disorders (Frazzini et al. 2016; Gilani et al. 2014; Jones et al. 2016; Palop and Mucke 2016; Schmitz et al. 2017; Schobel et al. 2013). This hypothesis finds some support by the combined analysis of the MCI subgroups. We find that the hyper-connectivity of nc-MCI subjects is inhibited by the presence of the AD-related pathology as, out of a total of 54 nC-MCI subjects, the phenomenon is missing in 25 who are AD^+ (**Suppl. Fig. 2**). On the other hand, in our MCI set, the presence of the AD-related pathology is not sufficient, at least in the two-year timeframe of the dataset, to promote the conversion to AD. A crossed analysis (nc/c; AD+/-) shows in fact that as, out of a total of 37 nc-MCI subjects, 25 are also AD^+, a finding that is in line with the current view of AD as a multifactorial condition driven by amyloid-dependent and independent mechanisms.

Further investigations, combining proton MR spectroscopy and rs-fMRI, will be needed to test this hypothesis and understand the nature and precise timeline of the functional changes occurring in MCI individuals along with their molecular underpinnings.

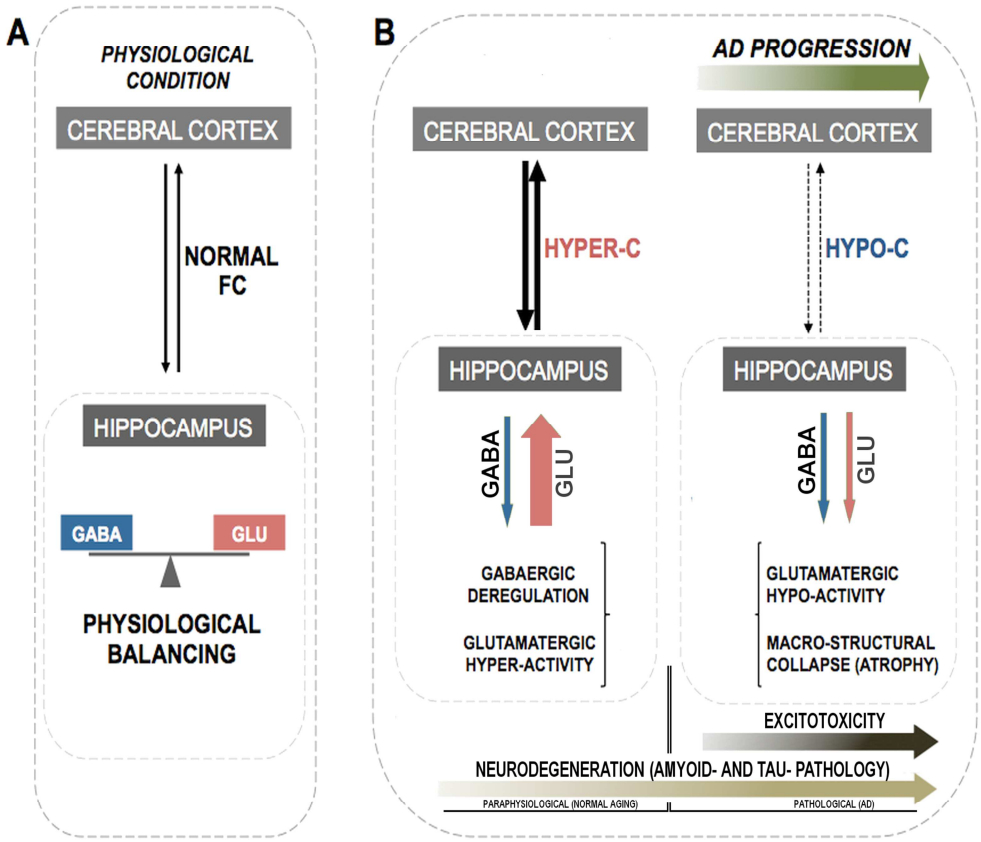

Figure 8. Proposed model of changes in hippocampal connectivity that occur at different stages of the AD spectrum. In MCI^{AD-} patients, the para-physiological occurrence of tau deposition, a phenomenon restricted to the MTL, may favor the down-regulation of GABAergic neurotransmission that can promote compensatory, cognitively-relevant, hyperexcitability. In MCI^{AD+} patients, the convergence of amyloid-dependent and independent mechanisms may favor the transition to widespread and patent tau pathology, thereby unleashing a glutamatergic overdrive, pathological hyperexcitability, excitotoxicity, micro/ macro-structural damage, atrophy, deficient hippocampal functioning, and the progression to cognitive and behavioral disorders.

5. Conclusions

The study identifies the functional correlates of alterations that occur in MCI patients. Our study has some limitations. For instance, the neuropsychological tests employed in the ADNI database

are skewed toward the investigation of mnemonic domains and do not allow a detailed analysis of visuospatial and attentional domains. The dataset does offer information on the longitudinal variations of the fMRI changes, an issue that should be addressed by future investigation. Finally, the model should be tested and further validated by investigating changes in functional and structural connectivity in relation to ongoing processes of amyloid and tau deposition, brain metabolism and synaptic density as assessed by PET imaging. The study nevertheless offers a functional biomarker that can be used in selected diagnostic settings and may indicate a window of therapeutic opportunity in subsets of MCI patients.

Acknowledgments

This work was supported by research grants from the Italian Department of Education (PRIN 2011; 2010M2JARJ_005), the Italian Department of Health (RF-2013–02358785 and NET-2011-02346784-1), and from the AIRAlzh Onlus (ANCC-COOP).

Data collection and sharing for this project was funded by the ADNI (National Institutes of Health Grant U01 AG024904). ADNI is funded by the National Institute on Aging, the National Institute of Biomedical Imaging and Bioengineering, and through generous contributions from the following: AbbVie, Alzheimer's Association; Alzheimer's Drug Discovery Foundation; Araclon Biotech; BioClinica, Inc.; Biogen; Bristol-Myers Squibb Company; CereSpir, Inc.; Cogstate; Eisai Inc.; Elan Pharmaceuticals, Inc.; Eli Lilly and Company; EuroImmun; F. Hoffmann-La Roche Ltd and its affiliated company Genentech, Inc.; Fujirebio; GE Healthcare; IXICO Ltd.;Janssen Alzheimer Immunotherapy Research & Development, LLC.; Johnson & Johnson Pharmaceutical Research & Development LLC.; Lumosity; Lundbeck; Merck & Co., Inc.;Meso Scale Diagnostics, LLC.; NeuroRx Research; Neurotrack Technologies; Novartis Pharmaceuticals Corporation; Pfizer Inc.; Piramal Imaging; Servier; Takeda Pharmaceutical Company; and Transition Therapeutics. The Canadian Institutes of Health Research is providing funds to support ADNI clinical sites in Canada. Private sector contributions are facilitated by the Foundation for the National Institutes of Health (www.fnih.org). The grantee organization is the Northern California Institute for Research and Education, and the study is coordinated by the Alzheimer's Therapeutic Research Institute at the University of Southern California. ADNI data are disseminated by the Laboratory for Neuro Imaging at the University of Southern California.

The authors are grateful to all the members of the Molecular Neurology Unit for helpful discussions and to Dr. Domenico Ciavardelli for helping with the statistical analysis.

Table 1. Demographic, neuropsychological, and clinical features - I model

	nc-MCI (N=54)	c-MCI (N=13)	ANOVA [d]		Post-hoc					
			F or μ_2	p-value	HC vs. nc-MCI	HC vs. c-MCI	nc-MCI vs. c-MCI	nc-MCI vs. AD	c-MCI vs. AD	HC vs. AD
Gender (% Male)	54%	69%	8.729	**0.021**	**0.011**	**0.007**	0.310	0.352	0.116	0.188
Age (y)	71.6±7.1	71.7±6.1	0.470	0.703	NA	NA	NA	NA	NA	NA
Education (y)	15.9±2.7	16.2±2.5	1.558	0.203	NA	NA	NA	NA	NA	NA
CDR-RS	1.2±0.7	2.8±1.0	150.878	**<0.001**	**<0.001**	**<0.001**	**<0.001**	**<0.001**	**0.012**	**<0.001**
MMSE	27.9±1.7	27.0±1.6	55.520	**<0.001**	**0.129**	**0.012**	0.667	**<0.001**	**<0.001**	**<0.001**
MOCA	23.1±3.2	22.6±2.5	41.567	**<0.001**	**0.038**	0.062	1.000	**<0.001**	**<0.001**	**<0.001**
LM	7.2±3.0	6.5±3.0	87.650	**<0.001**	**<0.001**	**<0.001**	1.000	**<0.001**	**<0.001**	**<0.001**
ADAS11	8.7±3.5	12.2±4.3	72.559	**<0.001**	0.084	**0.001**	0.114	**<0.001**	**<0.001**	**<0.001**
ADAS13	14.0±5.2	19.1±6.2	86.011	**<0.001**	**0.013**	**<0.001**	**0.046**	**<0.001**	**<0.001**	**<0.001**
FAQ	2.1±3.4	8.0±3.1	84.147	**<0.001**	0.157	**<0.001**	**<0.001**	**<0.001**	**<0.001**	**<0.001**
AF	18.7±4.8	17.8±4.5	17.733	**<0.001**	0.295	0.235	1.000	**<0.001**	**0.004**	**<0.001**
BNT	27.1±3.1	25.8±4.9	13.471	**<0.001**	0.740	0.229	1.000	**<0.001**	**0.041**	**<0.001**
TMTA[#]	37.7±14.9	44.0±18.0	25.197	**<0.001**	1.000	0.587	0.975	**<0.001**	**<0.001**	**<0.001**
TMTB	105.5±60.	144.4±85.	34.944	**<0.001**	1.000	**0.017**	0.080	**<0.001**	**<0.001**	**<0.001**
LDEL[##]	9.4±2.7	8.4±3.7	91.511	**<0.001**	**<0.001**	**<0.001**	1.000	**<0.001**	**<0.001**	**<0.001**
LIMM[##]	7.2±3.0	6.5±3.0	105.492	**<0.001**	**<0.001**	**<0.001**	1.000	**<0.001**	**<0.001**	**<0.001**
AVDELT[##]	35.9±9.6	30.2±4.5	38.838	**<0.001**	**<0.001**	**<0.001**	0.226	**<0.001**	0.057	**<0.001**
AVDEL30[##]	4.5±3.7	1.5±1.9	28.687	**<0.001**	**0.001**	**<0.001**	**0.011**	**<0.001**	1.000	**<0.001**
RAVLT[##]	11.0±3.0	9.7±2.3	35.416	**<0.001**	0.874	**0.002**	**0.005**	**<0.001**	**0.001**	**<0.001**
APOE ε4	37%	62%	15.428	**0.001**	0.415	0.082	0.274	**0.004**	0.622	**0.001**
Aβ (pg/ml)[###]	1246±601	727±357	8.976	**<0.001**	1.000	**0.003**	**0.023**	**0.003**	1.000	**0.002**
tau (pg/ml)[###]	273±119	389±160	7.757	**<0.001**	1.000	**0.003**	**0.017**	**0.015**	1.000	**0.002**
p-Tau (pg/ml)[###]	25.4±12.5	39±19	8.294	**<0.001**	1.000	**0.001**	**0.004**	**0.017**	1.000	**0.003**
t-Tau/Aβ[###]	0.29±0.24	0.65±0.47	13.494	**<0.001**	1.000	**<0.001**	**0.001**	**0.001**	1.000	**<0.001**
p-Tau/Aβ[###]	0.03±0.02	0.07±0.05	9.843	**<0.001**	1.000	**0.001**	**0.003**	**0.002**	1.000	**0.004**
L-HP/eTIV [a,b]	2.47±0.44	2.28	15.710	**<0.001**	0.449	0.062	0.961	**<0.001**	0.056	**<0.001**
R-HP/eTIV [a,b]	2.56±0.46	2.23±0.53	14.620	**<0.001**	0.940	**0.008**	0.110	**<0.001**	0.679	**<0.001**
eTIV (mm^3)[c]	1.51±0.21	1.56±0.23	0.442	0.723	NA	NA	NA	NA	NA	NA
L-EC (mm)	3.31±0.48	3.21±0.63	12.225	**<0.001**	0.601	0.463	1.000	**<0.001**	0.058	**<0.001**
R-EC (mm)	3.42±0.41	3.04±0.63	10.729	**<0.001**	1.000	**0.014**	**0.039**	**<0.001**	1.000	**<0.001**

Values are expressed as the mean ± standard deviation (SD). [##] Data on episodic memory tests were available for 1 nc-MCI patient. [##] Data on CSF biomarkers were available for 46 nc-MCI patients and 13 c-MCI patients. [a] right (R) and left (L) hippocampus (HP) volumes are normalized for estimated total intracranial volume (eTIV); [b] values x 10^{-3}; [c] values x 10^6; [d] I model: comparison between HC, nc-MCI, c-MCI, and AD.

Abbreviations: ADAS=AD Assessment Scale; AF=Animal Fluency; BNT=Boston Naming Test; CDR-RS=Clinical Dementia Rating Scale; AVDELT= Rey Auditory Verbal Learning Test-Delayed Recognition Score; AVDEL30=Rey Auditory Verbal Learning Test-Delayed 30 Minute Delay Total; EC=entorhinal cortex; eTIV=estimated total intracranial volume; FAQ= Functional Activities Questionnaire; LDEL= Logical Memory-Delayed Recall Total Number of Story Units Recalled; LIMM=Logical Memory-Immediate Recall Total Number of Story Units Recalled; MMSE=Mini-Mental State Examination; MoCA=Montreal Cognitive Assessment; TMT=Trail Making Test; $A\beta_{1-42}$=amyloid β_{1-42}; p-Tau_{181}=tau phosphorylated at threonine 181; RAVLT=Rey Auditory Verbal Learning Test Immediate.

Table 2. Demographic, neuropsychological, and clinical features - II model

	MCI^{AD-} (N=22, 50% Male)	MCI^{AD+} (N=37, 64% Male)	ANOVA [d]		Post-hoc				
			F or μ_2	p-value	HC vs. MCI^{AD-}	HC vs. MCI^{AD+}	MCI^{AD-} vs. MCI^{AD+}	MCI^{AD-} vs. AD	MCI^{AD+} vs. AD
Age (y)	72±5.8	71.5±8	1.023	0.385	NA	NA	NA	NA	NA
Education (y)	16.2±2.5	15.5±2.7	1.523	0.212	0.726	1.000	0.378	1.000	1.000
CDR-RS	1.9±1.1	1.1±0.8	131.4	**<0.001**	**<0.001**	**<0.001**	**0.020**	**<0.001**	**<0.001**
MMSE	27.4±1.8	28.3±1.7	66.3	**<0.001**	1.000	**0.002**	0.375	**<0.001**	**<0.001**
MOCA	23±3.1	23.5±2.8	50.1	**<0.001**	0.084	**0.004**	1.000	**<0.001**	**<0.001**
LM	6.7±3	7.7±2.6	109.8	**<0.001**	**<0.001**	**<0.001**	1.000	**<0.001**	**<0.001**
ADAS11	10.2±4.4	8.3±3.3	73.2	**<0.001**	0.462	**0.002**	0.933	**<0.001**	**<0.001**
ADAS13	16±6.3	13.1±5.3	85.8	**<0.001**	0.213	**<0.001**	0.534	**<0.001**	**<0.001**
FAQ	4.3±4.7	2±2.9	76.0	**<0.001**	0.603	**<0.001**	**<0.001**	0.331	0.331
AF	18.6±4.6	18.9±5	15.2	**<0.001**	0.911	0.340	0.340	1.000	1.000
BNT	26.5±3.9	27.4±2.1	14.9	**<0.001**	1.000	0.119	1.000	**<0.001**	**<0.001**
TMTA	37±13.7	38.9±16.6	21.9	**<0.001**	1.000	1.000	1.000	**<0.001**	**<0.001**
TMTB	111.4±60.9	100.4±55.9	31.9	**<0.001**	1.000	0.633	1.000	**<0.001**	**<0.001**
LDELT	8.8±3.2	9.8±2.6	87.9	**<0.001**	**<0.001**	**<0.001**	1.000	**<0.001**	**<0.001**
LIMM	6.7±3	7.7±2.6	109.8	**<0.001**	**<0.001**	**<0.001**	1.000	**<0.001**	**<0.001**
AVDELT	33.8±7.9	35.3±10.3	36.2	**<0.001**	**<0.001**	**<0.001**	1.000	**<0.001**	**<0.001**
AVDEL30	3.4±3.5	4.3±3.7	24.6	**<0.001**	**0.010**	**<0.001**	1.000	**<0.001**	**0.002**
RAVLT	10.2±3.1	11.5±2.5	36.0	**<0.001**	0.265	**<0.001**	0.490	**<0.001**	**<0.001**
L-HP/eTIV [a,b]	2.25±0.43	2.23±0.37	14.8	**<0.001**	1.000	**0.026**	0.203	**0.004**	**1.000**
R-HP/eTIV [a,b]	2.64±0.44	2.24±0.43	11.7	**<0.001**	1.000	**0.019**	0.087	**<0.001**	0.075
eTIV (mm^3) [c]	1.49±0.18	1.55±0.21	0.69	0.560	NA	NA	NA	NA	NA
L-EC (mm)	3.36±0.52	3.20±0.48	12.1	**<0.001**	1.000	0.087	1.000	**<0.001**	**0.004**
R-EC (mm)	3.48±0.42	3.24±0.51	9.0	**<0.001**	1.000	0.173	0.310	**<0.001**	0.060

Values are expressed as the mean ± standard deviation (SD). [a] right (R) and left (L) hippocampus (HP) volumes are normalized for the estimated total intracranial volume (eTIV); [b] values x 10^{-3}; [c] values x 10^{6}; [d] II model: comparison between HC, MCI^{AD-}, MCI^{AD+}, and AD. Note: the comparison between HC and AD is also reported in Table 2.
Abbreviations: ADAS=AD Assessment Scale; AF=Animal Fluency; BNT=Boston Naming Test; CDR-RS=Clinical Dementia Rating Scale; AVDELT= Rey Auditory Verbal Learning Test-Delayed Recognition Score; AVDEL30=Rey Auditory Verbal Learning Test-Delayed 30 Minute Delay Total; EC=entorhinal cortex; eTIV=estimated total intracranial volume; FAQ= Functional Activities Questionnaire; LDEL= Logical Memory-Delayed Recall Total Number of Story Units Recalled; LIMM=Logical Memory-Immediate Recall Total Number of Story Units Recalled; MMSE=Mini-Mental State Examination; MoCA=Montreal Cognitive Assessment; TMT=Trail Making Test; RAVLT=Rey Auditory Verbal Learning Test Immediate.

Table 3. Longitudinal variations of the clinical and neuropsychological test scores of the MCI subsets.

	nc-MCI	c-MCI
MMSE	0.36±2.59	2.75±4.25
MOCA [#]	-0.28±2.87	4.17±4.06
AF [#]	0.56±4.28	6.00±4.26
BNT [#]	-0.46±1.92	2.25±2.99
TMTA	-0.57±11.78	11.23±24.06
TMTB	1.70±52.14	77.46±84.86
LDEL [#]	-0.32±3.26	3.50±2.43
LIMM[#]	-0.44±4.05	3.42±3.06
AVDELT [#]	0.22±6.93	5.83±9.77
AVDEL30 [#]	0.71±3.10	1.25±1.96
RAVLT [#]	0.71±3.34	0.42±3.06

Values are expressed as the mean ± standard deviation (SD).
[#] Longitudinal data on episodic memory tests were available for 92% of the MCI sample. *Abbreviations:* AF=Animal Fluency; BNT=Boston Naming Test; AVDELT= Rey Auditory Verbal Learning Test-Delayed Recognition Score; AVDEL30=Rey Auditory Verbal Learning Test-Delayed 30 Minute Delay Total; LDEL= Logical Memory-Delayed Recall Total Number of Story Units Recalled; LIMM=Logical Memory-Immediate Recall

Table 4. Relationships between FC strength and longitudinal changes in cognition.

FC strength of R-HP with	Statistics	MMSE	MOCA	AF	BNT	TMTA	TMTB	LDEL	LIMM	AVDELT	AVDEL30	RAVLT
L-mPFC	Corr. Coeff.	0.019	-0.201	-0.093	**-0.305***	**-0.241***	-0.087	0.075	-0.136	-0.074	-0.102	0.025
	p-value	0.885	0.116	0.472	**0.016**	**0.050**	0.482	0.562	0.293	0.570	0.433	0.849
R-mPFC	Corr. Coeff.	-0.061	**-0.217**	-0.066	**-0.267***	-0.148	-0.050	0.070	-0.082	-0.075	**-0.222**	0.059
	p-value	0.637	**0.091**	0.609	**0.036**	0.232	0.686	0.590	0.529	0.566	**0.086**	0.649

An asterisk indicates statistical significance. *Abbreviations:* AVDELT= Rey Auditory Verbal Learning Test-Delayed Recognition Score; AVDEL30=Rey Auditory Verbal Learning Test-Delayed 30 Minute Delay Total; AF=Animal Fluency; BNT=Boston Naming Test; FC=functional connectivity; HP=hippocampus; L=left; LDEL= Logical Memory-Delayed Recall Total Number of Story Units Recalled; LIMM=Logical Memory-Immediate Recall Total Number of Story Units Recalled; MMSE=Mini-Mental State Examination; MOCA=Montreal-Cognitive Assessment; R=right; RAVLT=Rey Auditory Verbal Learning Total Number of Story Units Recalled; MMSE=Mini-Mental State Examination; MoCA=Montreal Cognitive Assessment; TMT=Trail Making Test; RAVLT=Rey Auditory Verbal Learning.

References

Alsop DC, Casement M, de Bazelaire C, et al. Hippocampal hyperperfusion in Alzheimer's disease. Neuroimage 2008; 42:1267-74.

Alsop DC, Dai W, Grossman M, et al. Arterial spin labeling blood flow MRI: its role in the early characterization of Alzheimer's disease. J Alzheimers Dis 2010; 20:871-80.

Apostolova LG, Dutton RA, Dinov ID, et al. Conversion of mild cognitive impairment to Alzheimer disease predicted by hippocampal atrophy maps. Archives of neurology 2006;63:693-9.

Badhwar A, Tam A, Dansereau C, et al. Resting-state network dysfunction in Alzheimer's disease: A systematic review and meta-analysis. Alzheimer's & dementia 2017;8:73-85.

Barker GR, Bird F, Alexander V, et al. Recognition memory for objects, place, and temporal order: a disconnection analysis of the role of the medial prefrontal cortex and perirhinal cortex. J Neurosci 2007;27:2948-57.

Bondi MW, Houston WS, Eyler LT, et al. fMRI evidence of compensatory mechanisms in older adults at genetic risk for Alzheimer disease. Neurology 2005;64:501-8.

Braak E, Braak H, Mandelkow EM. A sequence of cytoskeleton changes related to the formation of neurofibrillary tangles and neuropil threads. Acta neuropathologica 1994;87:554-7.

Braak H, Feldengut S, Del Tredici K. [Pathogenesis and prevention of Alzheimer's disease: when and in what way does the pathological process begin?]. Der Nervenarzt 2013;84:477-82.

Buckner RL, Krienen FM, Castellanos A, et al. The organization of the human cerebellum estimated by intrinsic functional connectivity. Journal of neurophysiology 2011;106:2322-45.

Buckner RL, Snyder AZ, Shannon BJ, et al. Molecular, structural, and functional characterization of Alzheimer's disease: evidence for a relationship between default activity, amyloid, and memory. J Neurosci 2005;25:7709-17.

Busse A, Hensel A, Guhne U, et al. Mild cognitive impairment: long-term course of four clinical subtypes. Neurology 2006;67:2176-85.

Cabeza R, Grady CL, Nyberg L, et al. Age-related differences in neural activity during memory encoding and retrieval: a positron emission tomography study. J Neurosci 1997;17:391-400.

Canto CB, Wouterlood FG, Witter MP. What does the anatomical organization of the entorhinal cortex tell us? Neural Plast 2008;2008:381243.

Canuet L, Pusil S, Lopez ME, et al. Network Disruption and Cerebrospinal Fluid Amyloid-Beta and Phospho-Tau Levels in Mild Cognitive Impairment. J Neurosci 2015;35:10325-30.

Cope TE, Rittman T, Borchert RJ, et al. Tau burden and the functional connectome in Alzheimer's disease and progressive supranuclear palsy. Brain 2018;141:550-67.

Dai W, Lopez OL, Carmichael OT, et al. Mild cognitive impairment and Alzheimer's disease: patterns of altered cerebral blood flow at MR imaging. Radiology 2009;250:856-66.

Das SR, Pluta J, Mancuso L, et al. Increased functional connectivity within medial temporal lobe in mild cognitive impairment. Hippocampus 2013;23:1-6.

Davis SW, Dennis NA, Daselaar SM, et al. Que PASA? The posterior-anterior shift in aging. Cereb Cortex 2008;18:1201-9.

Desikan RS, Segonne F, Fischl B, et al. An automated labeling system for subdividing the human cerebral cortex on MRI scans into gyral based regions of interest. Neuroimage 2006;31:968-80.

Dickerson BC, Sperling RA. Functional abnormalities of the medial temporal lobe memory system in mild cognitive impairment and Alzheimer's disease: insights from functional MRI studies. Neuropsychologia 2008;46:1624-35.

Drzezga A, Becker JA, Van Dijk KR, et al. Neuronal dysfunction and disconnection of cortical hubs in non-demented subjects with elevated amyloid burden. Brain 2011;134:1635-46.

Eichenbaum H. 2017. Memory: Organization and Control. Annual review of psychology 68:19-45.

Elman JA, Madison CM, Baker SL, et al. Effects of Beta-Amyloid on Resting State Functional Connectivity Within and Between Networks Reflect Known Patterns of Regional Vulnerability. Cereb Cortex 2016;26:695-707.

Fabiani M. It was the best of times, it was the worst of times: a psychophysiologist's view of cognitive aging. Psychophysiology 2012;49:283-304.

Ferraris M, Ghestem A, Vicente AF, et al. The Nucleus Reuniens Controls Long-Range Hippocampo-Prefrontal Gamma Synchronization during Slow Oscillations. J Neurosci 2018;38:3026-38.

Fischl B, Salat DH, van der Kouwe A, et al. Sequence-independent segmentation of magnetic resonance images. NeuroImage 2004;23: pp. S69-84.

Folstein MF, Folstein SE, McHugh PR. "Mini-mental state". A practical method for grading the cognitive state of patients for the clinician. Journal of psychiatric research 1975;12:189-98.

Foster CM, Kennedy KM, Horn MM, et al. Both hyper- and hypo-activation to cognitive challenge are associated with increased beta-amyloid deposition in healthy aging: A nonlinear effect. Neuroimage 2018;166:285-92.

Frazzini V, Guarnieri S, Bomba M, et al. Altered Kv2.1 functioning promotes increased excitability in hippocampal neurons of an Alzheimer's disease mouse model. Cell Death Dis. 2016;7:e2100.

Frisoni GB, Jessen F. One step towards dementia prevention. Lancet Neurol 2018;17:294-5.

Gilani AM, Knowles TG, Nicol CJ. Factors affecting ranging behaviour in young and adult laying hens. British poultry science 2014;55:127-35.

Gomez-Isla T, Price JL, McKeel DW, Jr., et al. Profound loss of layer II entorhinal cortex neurons occurs in very mild Alzheimer's disease. J Neurosci 1996;16:4491-500.

Grothe MJ, Teipel SJ, Alzheimer's Disease Neuroimaging I. Spatial patterns of atrophy, hypometabolism, and amyloid deposition in Alzheimer's disease correspond to dissociable functional brain networks. Human brain mapping 2016;37:35-53.

Grundman M, Sencakova D, Jack CR Jr, et al. Brain MRI hippocampal volume and prediction of clinical status in a mild cognitive impairment trial. Journal of molecular neuroscience 2002;19:23-27.

Hagler DJ Jr, Saygin AP, Sereno MI. Smoothing and cluster thresholding for cortical surface-based group analysis of fMRI data. Neuroimage 2006;33:1093-103.

Hellyer PJ, Shanahan M, Scott G, et al. The control of global brain dynamics: opposing actions of frontoparietal control and default mode networks on attention. J Neurosci 2014;34:451-61.

Henneman WJ, Sluimer JD, Barnes J, et al. Hippocampal atrophy rates in Alzheimer disease: added value over whole brain volume measures. Neurology 2009;72:999-1007.

Hillary FG, Grafman JH. Injured Brains and Adaptive Networks: The Benefits and Costs of Hyperconnectivity. Trends in cognitive sciences 2017;21:385-401.

Hoenig MC, Bischof GN, Seemiller J, et al. Networks of tau distribution in Alzheimer's disease. Brain 2018;141:568-81.

Huijbers W, Mormino EC, Schultz AP, et al. Amyloid-beta deposition in mild cognitive impairment is associated with increased hippocampal activity, atrophy and clinical progression. Brain 2015; 138:1023-35.

Jack CR Jr, Shiung MM, Gunter JL, et al. Comparison of different MRI brain atrophy rate measures with clinical disease progression in AD. Neurology 2004;62:591-600.

Jack CR Jr, Bennett DA, Blennow K, et al. A/T/N: an unbiased descriptive classification scheme for Alzheimer disease biomarkers. Neurology 2016; 87: pp. 539-47.

Johnson KA, Shultz A, Betensky RA, et al. Tau positron emission tomographic imaging in aging and early Alzheimer's disease. Ann Neurol 2016;79: 110-9.

Jones DT, Knopman DS, Gunter JL, et al. Cascading network failure across the Alzheimer's disease spectrum. Brain 2016; 139:547-562.

Kahn I, Andrews-Hanna JR, Vincent JL, et al. Distinct cortical anatomy linked to subregions of the medial temporal lobe revealed by intrinsic functional connectivity. Journal of neurophysiology 2008;100:129-39.

Kaplan E GH, Weintraub S, editors. The Boston Naming Test. In: Philadelphia, PA. Lea & Febiger; 1983.

Kircher TT, Weis S, Freymann K, et al. Hippocampal activation in patients with mild cognitive impairment is necessary for successful memory encoding. J Neurol Neurosurg Psychiatry 2007;78:812-8.

Koch W, Teipel S, Mueller S, et al. Effects of aging on default mode network activity in resting state fMRI: does the method of analysis matter? Neuroimage 2010;51:280-7.

Lacy JW, Stark CE. Intrinsic functional connectivity of the human medial temporal lobe suggests a distinction between adjacent MTL cortices and hippocampus. Hippocampus 2012;22:2290-302.

Levenga J, Krishnamurthy P, Rajamohamedsait H, et al. Tau pathology induces loss of GABAergic interneurons leading to altered synaptic plasticity and behavioral impairments. Acta Neuropathol Commun 2013;1:34.

Libby LA, Ekstrom AD, Ragland JD, Ranganath C. Differential connectivity of perirhinal and parahippocampal cortices within human hippocampal subregions revealed by high-resolution functional imaging. J Neurosci 2012;32:6550-60.

Lo RY, Jagust WJ. and Alzheimer's Disease Neuroimaging Initiative. Effect of cognitive reserve markers on Alzheimer pathologic progression. Alzheimer Dis Assoc Disord 2013;27:343-50.

Mitchell AJ, Shiri-Feshki M. Rate of progression of mild cognitive impairment to dementia--meta-analysis of 41 robust inception cohort studies. Acta psychiatrica Scandinavica 2009; 119:252-65.

Mohs RC, Cohen L. Alzheimer's Disease Assessment Scale (ADAS). Psychopharmacology bulletin 1988;24:627-8.

Mohs RC, Knopman D, Petersen RC, et al. Development of cognitive instruments for use in clinical trials of antidementia drugs: additions to the Alzheimer's Disease Assessment Scale that broaden its scope.

The Alzheimer's Disease Cooperative Study. Alzheimer disease and associated disorders 1997;11 Suppl 2:S13-21.

Mormino EC, Smiljic A, Hayenga AO, et al. Relationships between beta-amyloid and functional connectivity in different components of the default mode network in aging. Cereb Cortex 2011;21:2399-407.

Morris JC. The Clinical Dementia Rating (CDR): current version and scoring rules. Neurology 1993; 43:2412-4.

Morris JC, Heyman A, Mohs RC, et al. The Consortium to Establish a Registry for Alzheimer's Disease (CERAD). Part I. Clinical and neuropsychological assessment of Alzheimer's disease. Neurology 1989;39:1159-65.

Mueller SG, Schuff N, Yaffe K, et al. Hippocampal atrophy patterns in mild cognitive impairment and Alzheimer's disease. Hum Brain Mapp 2010;31:1339-47.

Mutlu J, Landeau B, Gaubert M, et al. Distinct influence of specific versus global connectivity on the different Alzheimer's disease biomarkers. Brain 2017;140:3317-28.

Nasreddine ZS, Phillips NA, Bedirian V, et al. The Montreal Cognitive Assessment, MoCA: a brief screening tool for mild cognitive impairment. Journal of the American Geriatrics Society 2005;53:695-9.

Oh H, Jagust WJ. Frontotemporal network connectivity during memory encoding is increased with aging and disrupted by beta-amyloid. J Neurosci 2013;33:18425-37.

Ossenkoppele R, Schonhaut DR, Schöll M, et al. Tau PET patterns mirror clinical and neuroanatomical variability in Alzheimer's disease. Brain 2016;139(pt 5):1551-67.

Palop JJ, Mucke L. Network abnormalities and interneuron dysfunction in Alzheimer disease. Nat Rev Neurosci 2016;17:777-92.

Palmqvist S, Scholl M, Strandberg O, et al. Earliest accumulation of beta-amyloid occurs within the default-mode network and concurrently affects brain connectivity. Nat Commun 2017;8:1214.

Park DC, Reuter-Lorenz P. The adaptive brain: aging and neurocognitive scaffolding. Annual review of psychology 2009;60:173-96.

Pasquini L, Scherr M, Tahmasian M, Meng C, Myers NE, Ortner M, Muhlau M, Kurz A, Forstl H, Zimmer C, Grimmer T, Wohlschlager AM, Riedl V, Sorg C. Link between hippocampus' raised local and eased global intrinsic connectivity in AD. Alzheimers Dement 2015;11:475-84.

Petersen RC, Aisen PS, Beckett LA, Donohue MC, Gamst AC, Harvey DJ, Jack CR, Jr., Jagust WJ, Shaw LM, Toga AW, Trojanowski JQ, Weiner MW. Alzheimer's Disease Neuroimaging Initiative (ADNI): clinical characterization. Neurology 2010;74:201-9.

Pfeffer RI, Kurosaki TT, Harrah CH Jr, et al. Measurement of functional activities in older adults in the community. Journal of gerontology 1982;37:323-9.

Preston AR, Eichenbaum H. Interplay of hippocampus and prefrontal cortex in memory. Current biology 2013;23:764-773.

Putcha D, Brickhouse M, O'Keefe K, et al. Hippocampal hyperactivation associated with cortical thinning in Alzheimer's disease signature regions in non-demented elderly adults. J Neurosci 2011;31:17680-8.

Ranganath C, Ritchey M. Two cortical systems for memory-guided behaviour. Nat Rev Neurosci 2012;13:713-26.

Rey A. editor. L'examen clinique en psychologie, Presses Universitaires de France. Paris; 1964.

Reuter-Lorenz PA, Park DC. How does it STAC up? Revisiting the scaffolding theory of aging and cognition. Neuropsychology review 2014;24:355-70.

Schindler SE, Gray JD, Gordon BA, et al. Cerebrospinal fluid biomarkers measured by Elecsys assays compared to amyloid imaging. Alzheimers Dement 2018; In press.

Schmitz JM, Green CE, Hasan KM, et al. PPAR-gamma agonist pioglitazone modifies craving intensity and brain white matter integrity in patients with primary cocaine use disorder: a double-blind randomized controlled pilot trial. Addiction 2017;112:1861-8.

Schneider-Garces NJ, Gordon BA, Brumback-Peltz CR, et al. Span, CRUNCH, and beyond: working memory capacity and the aging brain. Journal of cognitive neuroscience 2010;22:655-69.

Schobel SA, Chaudhury NH, Khan UA, et al. Imaging patients with psychosis and a mouse model establishes a spreading pattern of hippocampal dysfunction and implicates glutamate as a driver. Neuron 2013;78:81-93.

Scholl M, Lockhart SN, Schonhaut DR, et al. PET Imaging of Tau Deposition in the Aging Human Brain. Neuron. 2016;89:971-82.

Schultz AP, Chhatwal JP, Hedden T, et al. Phases of Hyperconnectivity and Hypoconnectivity in the Default Mode and Salience Networks Track with Amyloid and Tau in Clinically Normal Individuals. J Neurosci 2017;37:4323-31.

Scimeca JM, Badre D. Striatal contributions to declarative memory retrieval. Neuron 2012; 75:380-92.

Sepulcre J, Sabuncu MR, Li Q, et al. Tau and amyloid beta proteins distinctively associate to functional network changes in the aging brain. Alzheimers Dement 2017;13:1261-9.

Sestieri C, Shulman GL, Corbetta M. The contribution of the human posterior parietal cortex to episodic memory. Nat Rev Neurosci 2017;18:183-92.

Sperling RA, Laviolette PS, O'Keefe K, et al. Amyloid deposition is associated with impaired default network function in older persons without dementia. Neuron 2009;63:178-88.

Sperling RA, Dickerson BC, Pihlajamaki M, et al. Functional alterations in memory networks in early Alzheimer's disease. Neuromolecular Med 2010;12:27-43.

Sperling R, Mormino E, Johnson K. The evolution of preclinical Alzheimer's disease: Implications for prevention trials. Neuron 2014; 84:608-622.

Spreen O SE. Compendium of neuropsychological tests. In: New York: Oxford University Press; 1998.

Stoodley CJ. The cerebellum and cognition: evidence from functional imaging studies. Cerebellum 2012;11:352-65.

Tabatabaei-Jafari H, Shaw ME, Cherbuin N. Cerebral atrophy in mild cognitive impairment: A systematic review with meta-analysis. Alzheimers Dement 2015; 1:487-504

Tulving E, Kapur S, Craik FI, et al. Hemispheric encoding/retrieval asymmetry in episodic memory: positron emission tomography findings. Proceedings of the National Academy of Sciences of the United States of America 1994;91:2016-20.

van den Heuvel MP, Sporns O. Rich-club organization of the human connectome. J Neurosci 2011;31:15775-86.

Vann SD, Aggleton JP, Maguire EA. What does the retrosplenial cortex do? Nat Rev Neurosci 2009;10:792-802.

Wechsler D. WMS-R Wechsler Memory Scale–Revised. San Antonio: The Psychological Corporation Harcourt Brace Jovanovich; 1987.

Wolk DA, Dunfee KL, Dickerson BC, et al. A medial temporal lobe division of labor: insights from memory in aging and early Alzheimer disease. Hippocampus 2011;21:461-66.

Yassa MA, Muftuler LT, Stark CE. Ultrahigh-resolution microstructural diffusion tensor imaging reveals perforant path degradation in aged humans in vivo. Proceedings of the National Academy of Sciences of the United States of America 2010a;107:12687-12691.

Yassa MA, Stark SM, Bakker A, et al. High-resolution structural and functional MRI of hippocampal CA3 and dentate gyrus in patients with amnestic Mild Cognitive Impairment. Neuroimage 2010b;51:1242-52.

Yassa MA, Mattfeld AT, Stark SM, et al. Age-related memory deficits linked to circuit-specific disruptions in the hippocampus. Proceedings of the National Academy of Sciences of the United States of America 2011;108:8873-78.

Yeo BT, Krienen FM, Sepulcre J, et al. The organization of the human cerebral cortex estimated by intrinsic functional connectivity. J Neurophysiol 2011;106:1125-65.

Yu W, Krook-Magnuson E. Cognitive Collaborations: Bidirectional Functional Connectivity Between the Cerebellum and the Hippocampus. Front Syst Neurosci 2015;9:177.

Yushkevich PA, Pluta JB, Wang H, et al. Hippocampal Subfields Group (HSG). Automated volumetry and regional thickness analysis of hippocampal subfields and medial temporal cortical structures in mild cognitive impairment. Hum Brain Mapp. 2015;36:258-87.

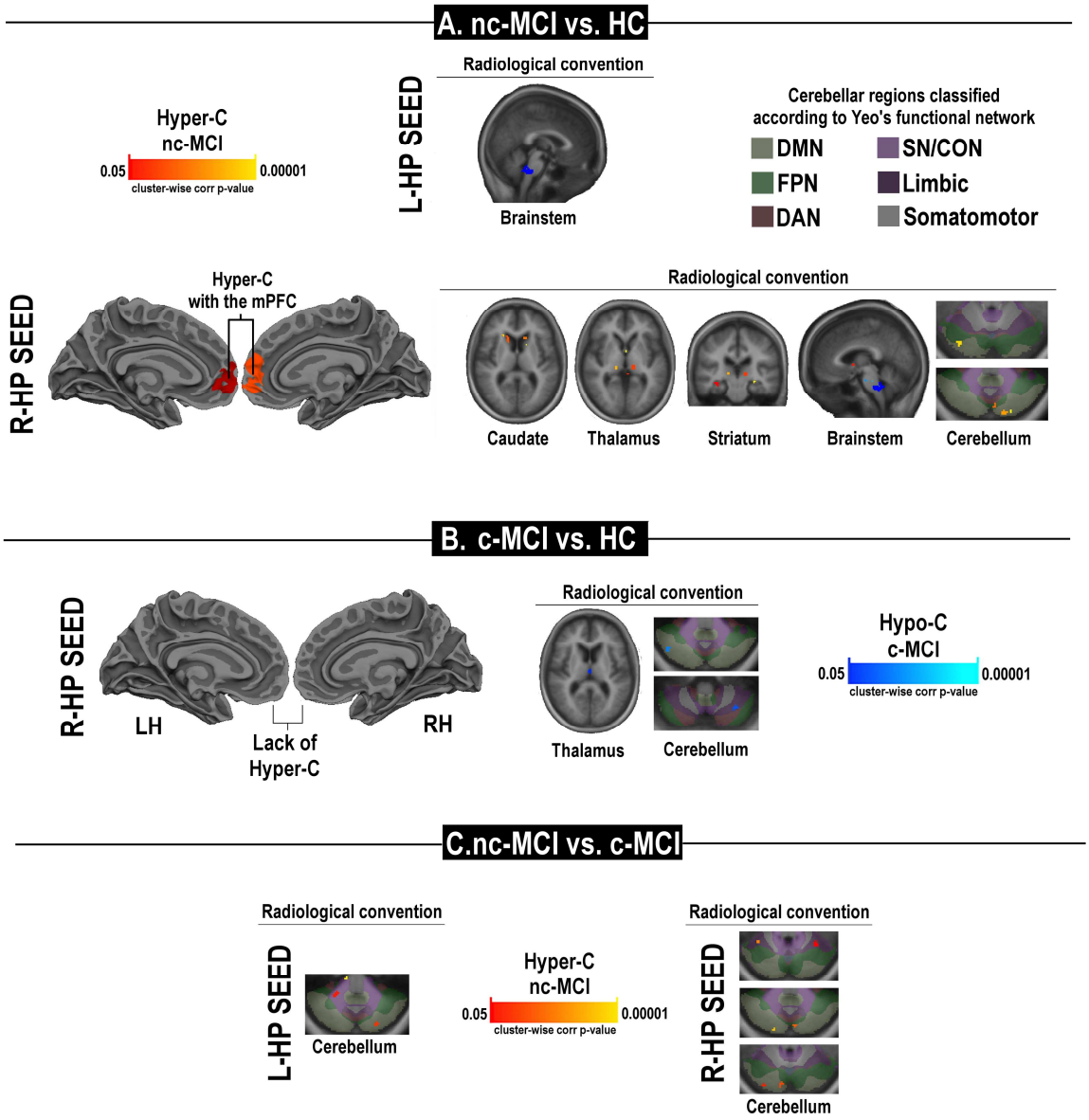

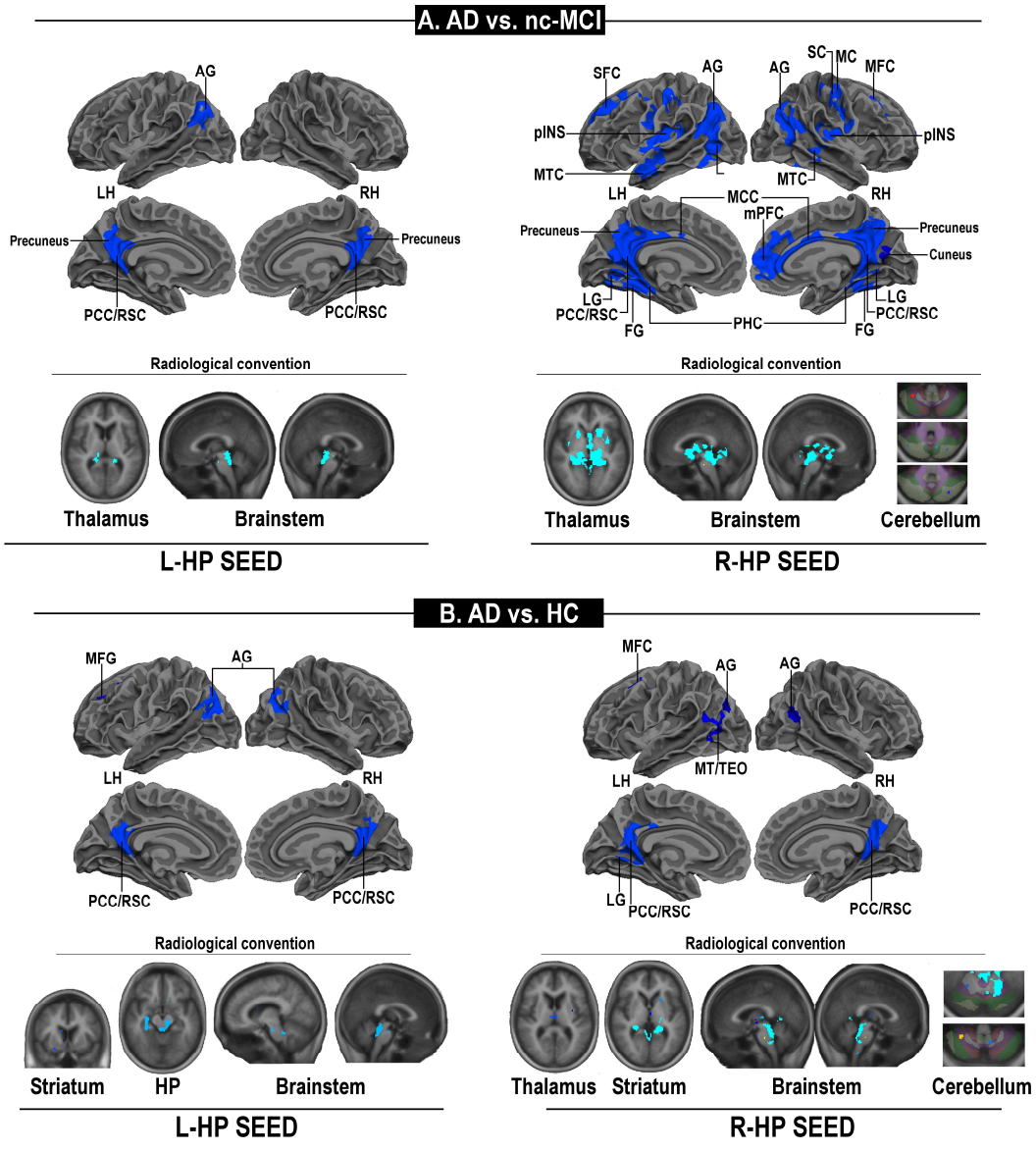
A. AD vs. nc-MCI
AG
LH
RH
Precuneus
Precuneus
PCC/RSC
PCC/RSC
SFC
AG
AG
SC
MC
MFC
pINS
pINS
MTC
MTC
LH
MCC
mPFC
RH
Precuneus
Precuneus
Cuneus
LG
PCC/RSC
FG
PHC
FG
LG
PCC/RSC
Radiological convention
Radiological convention
Thalamus
Brainstem
Thalamus
Brainstem
Cerebellum
L-HP SEED
R-HP SEED
B. AD vs. HC
MFG
AG
LH
RH
PCC/RSC
PCC/RSC
MFC
AG
AG
MT/TEO
LH
RH
LG
PCC/RSC
PCC/RSC
Radiological convention
Radiological convention
Striatum
HP
Brainstem
Thalamus
Striatum
Brainstem
Cerebellum
L-HP SEED
R-HP SEED
Hypo-C
AD
0.05
0.00001
cluster-wise corr p-value
Cerebellar regions classified
according to Yeo's functional network
DMN
SN/CON
FPN
Limbic
DAN
Somatomotor

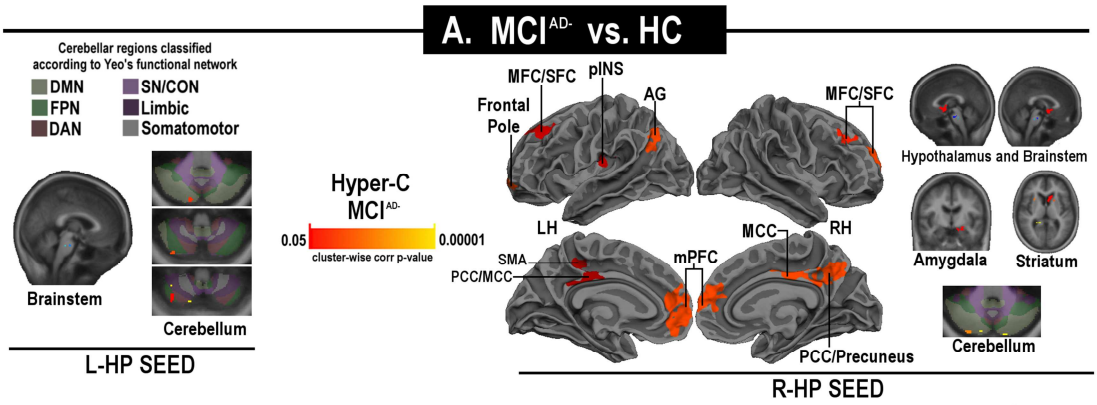
A. MCI AD- vs. HC
Cerebellar regions classified according to Yeo's functional network
DMN
SN/CON
FPN
Limbic
DAN
Somatomotor
Brainstem
Cerebellum
L-HP SEED
Hyper-C MCI AD-
0.05
0.00001
cluster-wise corr p-value
MFC/SFC
pINS
Frontal Pole
AG
MFC/SFC
Hypothalamus and Brainstem
LH
RH
MCC
SMA
mPFC
PCC/MCC
Amygdala
Striatum
Cerebellum
PCC/Precuneus
R-HP SEED

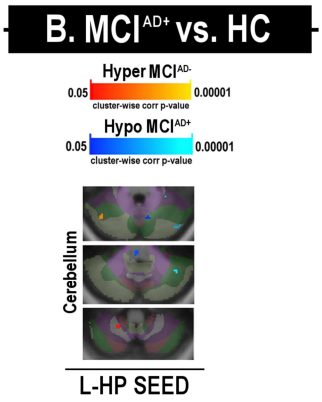
B. MCI AD+ vs. HC
Hyper MCI AD-
0.05
0.00001
cluster-wise corr p-value
Hypo MCI AD+
0.05
0.00001
cluster-wise corr p-value
Cerebellum
L-HP SEED

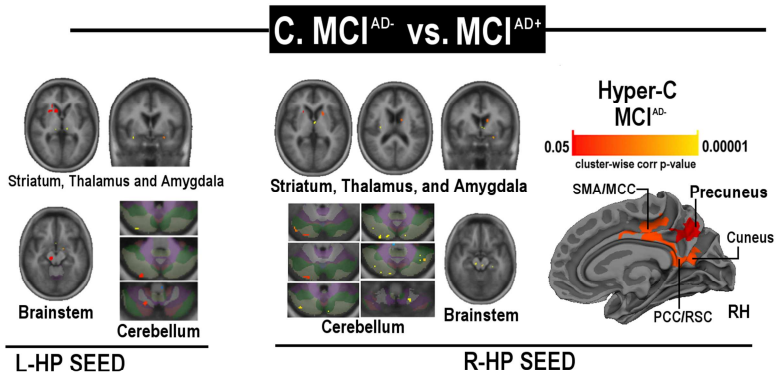
C. MCI AD- vs. MCI AD+
Striatum, Thalamus and Amygdala
Brainstem
Cerebellum
L-HP SEED
Striatum, Thalamus, and Amygdala
Hyper-C MCI AD-
0.05
0.00001
cluster-wise corr p-value
SMA/MCC
Precuneus
Cuneus
PCC/RSC
RH
Cerebellum
Brainstem
R-HP SEED

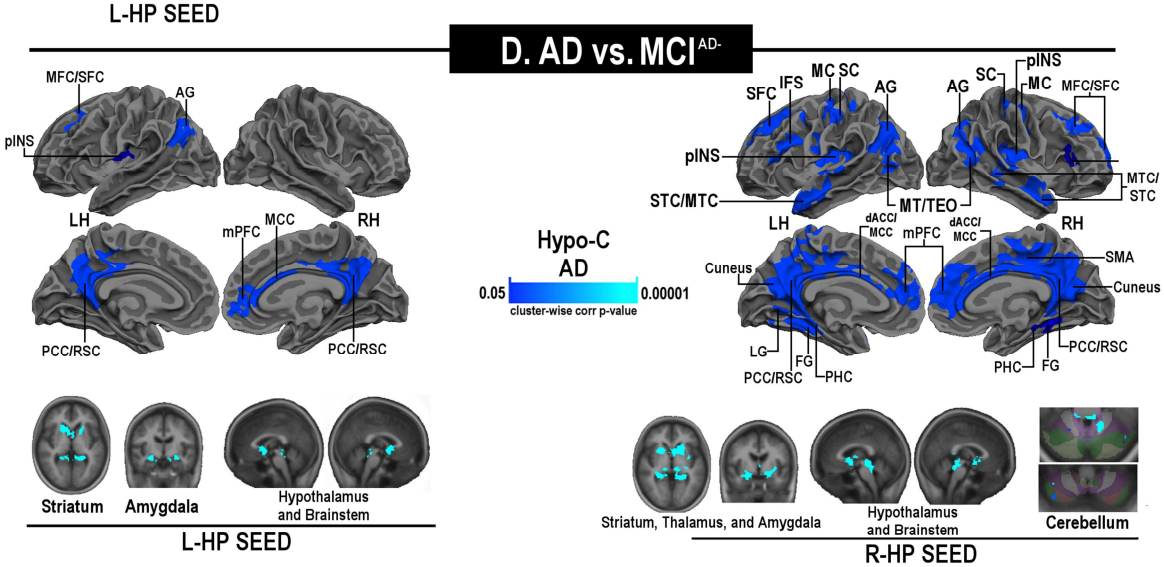
D. AD vs. MCI AD-
MFC/SFC
AG
pINS
LH
RH
mPFC
MCC
PCC/RSC
PCC/RSC
Striatum
Amygdala
Hypothalamus and Brainstem
L-HP SEED
Hypo-C AD
0.05
0.00001
cluster-wise corr p-value
SFC
IFS
MC
SC
AG
AG
SC
pINS
MC
MFC/SFC
pINS
STC/MTC
MT/TEO
MTC/STC
LH
dACC/MCC
mPFC
dACC/MCC
RH
SMA
Cuneus
Cuneus
LG
FG
PHC
PCC/RSC
PHC
FG
PCC/RSC
Striatum, Thalamus, and Amygdala
Hypothalamus and Brainstem
Cerebellum
R-HP SEED

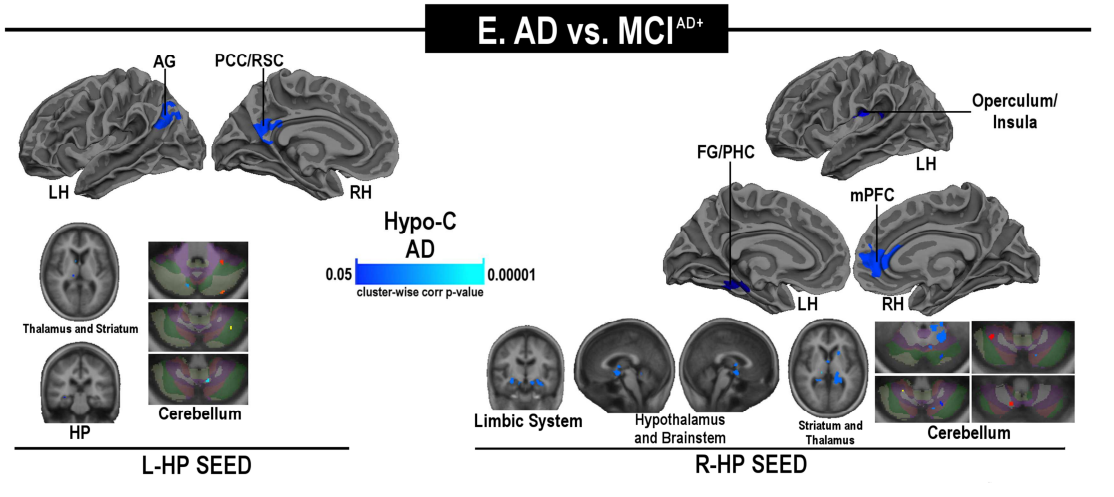
E. AD vs. MCI AD+
AG
PCC/RSC
LH
RH
Thalamus and Striatum
HP
Cerebellum
L-HP SEED
Hypo-C AD
0.05
0.00001
cluster-wise corr p-value
Operculum/Insula
FG/PHC
LH
mPFC
LH
RH
Limbic System
Hypothalamus and Brainstem
Striatum and Thalamus
Cerebellum
R-HP SEED

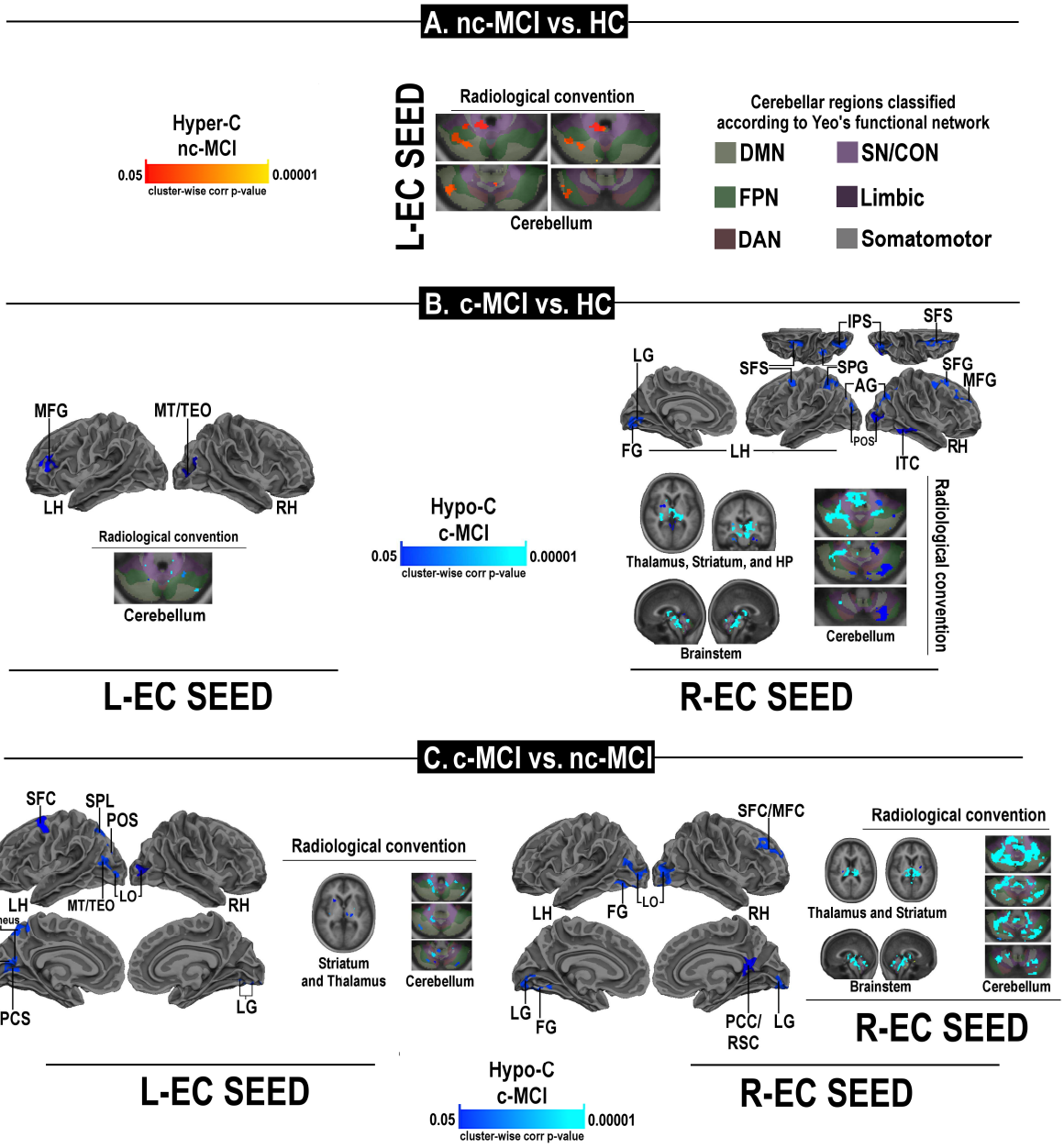
A. nc-MCI vs. HC
Hyper-C
nc-MCI
0.05
0.00001
cluster-wise corr p-value
L-EC SEED
Radiological convention
Cerebellum
Cerebellar regions classified
according to Yeo's functional network
DMN
SN/CON
FPN
Limbic
DAN
Somatomotor
B. c-MCI vs. HC
MFG
MT/TEO
LH
RH
Radiological convention
Cerebellum
L-EC SEED
Hypo-C
c-MCI
0.05
0.00001
cluster-wise corr p-value
IPS
SFS
LG
SFS
SPG
SFG
MFG
AG
FG
LH
POS
RH
ITC
Thalamus, Striatum, and HP
Brainstem
Cerebellum
Radiological convention
R-EC SEED
C. c-MCI vs. nc-MCI
SFC
SPL
POS
LH
MT/TEO
LO
RH
Precuneus
Cuneus
PCS
LG
Radiological convention
Striatum
and Thalamus
Cerebellum
L-EC SEED
SFC/MFC
LH
FG
LO
RH
LG
FG
PCC/
RSC
LG
Radiological convention
Thalamus and Striatum
Brainstem
Cerebellum
R-EC SEED
Hypo-C
c-MCI
0.05
0.00001
cluster-wise corr p-value
R-EC SEED

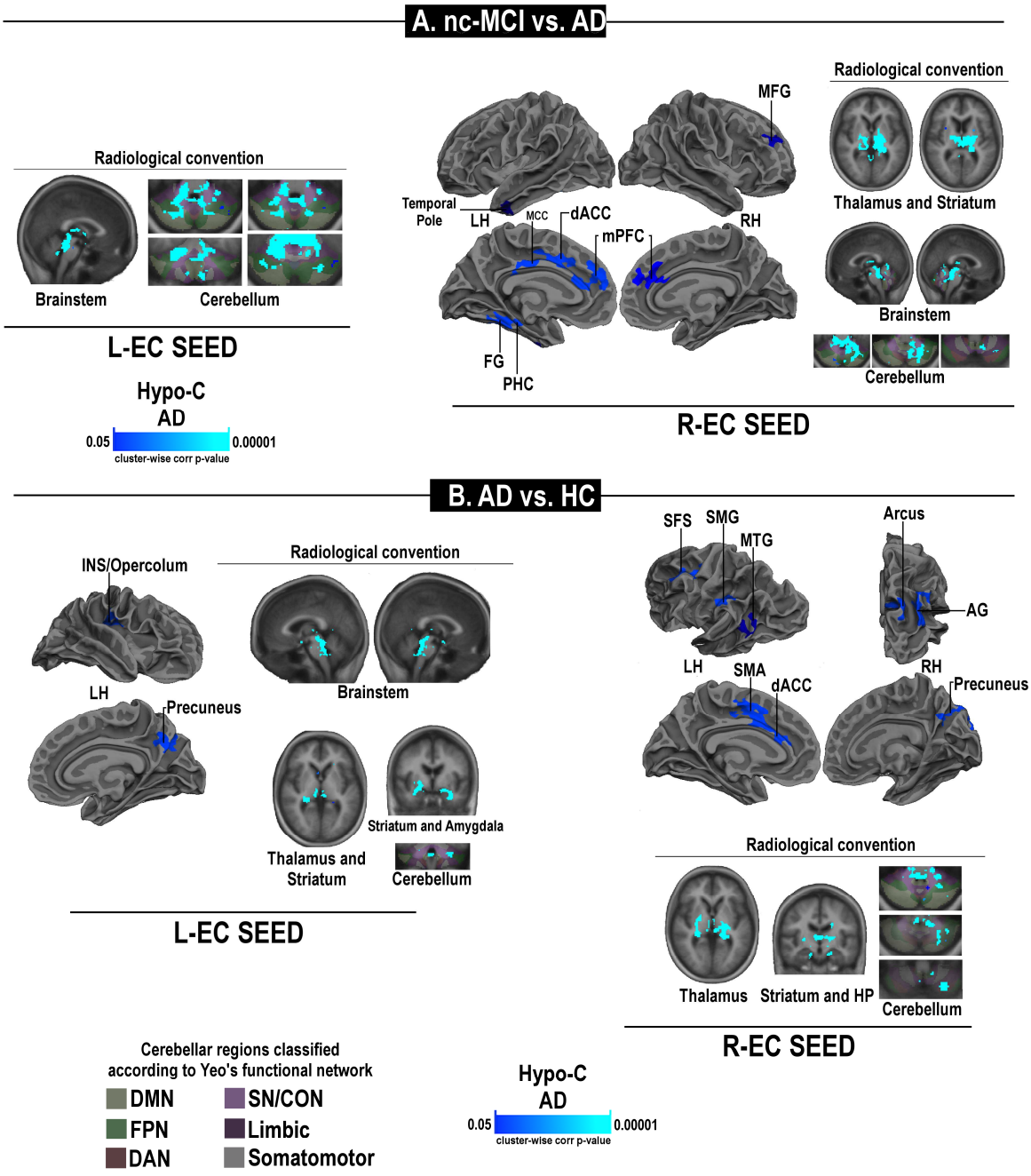
A. nc-MCI vs. AD
Radiological convention
Brainstem
Cerebellum
L-EC SEED
Hypo-C
AD
0.05
0.00001
cluster-wise corr p-value
MFG
Temporal Pole
LH
MCC
dACC
mPFC
RH
FG
PHC
Radiological convention
Thalamus and Striatum
Brainstem
Cerebellum
R-EC SEED
B. AD vs. HC
INS/Opercolum
Radiological convention
LH
Precuneus
Brainstem
Striatum and Amygdala
Thalamus and Striatum
Cerebellum
L-EC SEED
SFS
SMG
MTG
Arcus
AG
LH
SMA
dACC
RH
Precuneus
Radiological convention
Thalamus
Striatum and HP
Cerebellum
R-EC SEED
Cerebellar regions classified according to Yeo's functional network
DMN
SN/CON
FPN
Limbic
DAN
Somatomotor
Hypo-C
AD
0.05
0.00001
cluster-wise corr p-value

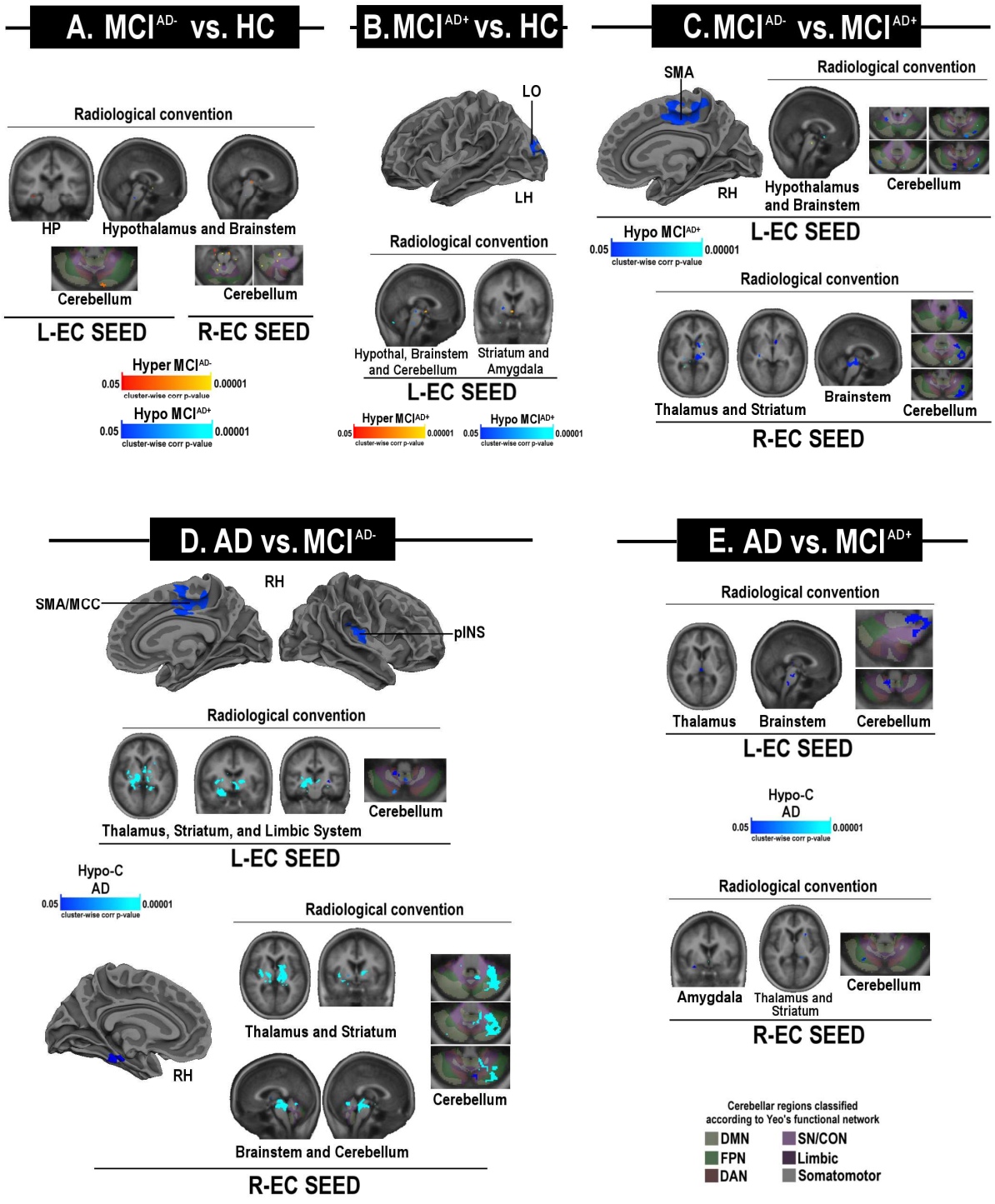
A. MCI AD- vs. HC
Radiological convention
HP
Hypothalamus and Brainstem
Cerebellum
Cerebellum
L-EC SEED
R-EC SEED
Hyper MCI AD-
0.05
0.00001
cluster-wise corr p-value
Hypo MCI AD+
0.05
0.00001
cluster-wise corr p-value
B. MCI AD+ vs. HC
LO
LH
Radiological convention
Hypothal, Brainstem and Cerebellum
Striatum and Amygdala
L-EC SEED
Hyper MCI AD+
0.05
0.00001
cluster-wise corr p-value
Hypo MCI AD+
0.05
0.00001
cluster-wise corr p-value
C. MCI AD- vs. MCI AD+
SMA
RH
Radiological convention
Hypothalamus and Brainstem
Cerebellum
Hypo MCI AD+
0.05
0.00001
cluster-wise corr p-value
L-EC SEED
Radiological convention
Thalamus and Striatum
Brainstem
Cerebellum
R-EC SEED
D. AD vs. MCI AD-
SMA/MCC
RH
pINS
Radiological convention
Cerebellum
Thalamus, Striatum, and Limbic System
L-EC SEED
Hypo-C AD
0.05
0.00001
cluster-wise corr p-value
Radiological convention
RH
Thalamus and Striatum
Cerebellum
Brainstem and Cerebellum
R-EC SEED
E. AD vs. MCI AD+
Radiological convention
Thalamus
Brainstem
Cerebellum
L-EC SEED
Hypo-C AD
0.05
0.00001
cluster-wise corr p-value
Radiological convention
Amygdala
Thalamus and Striatum
Cerebellum
R-EC SEED
Cerebellar regions classified according to Yeo's functional network
DMN
SN/CON
FPN
Limbic
DAN
Somatomotor

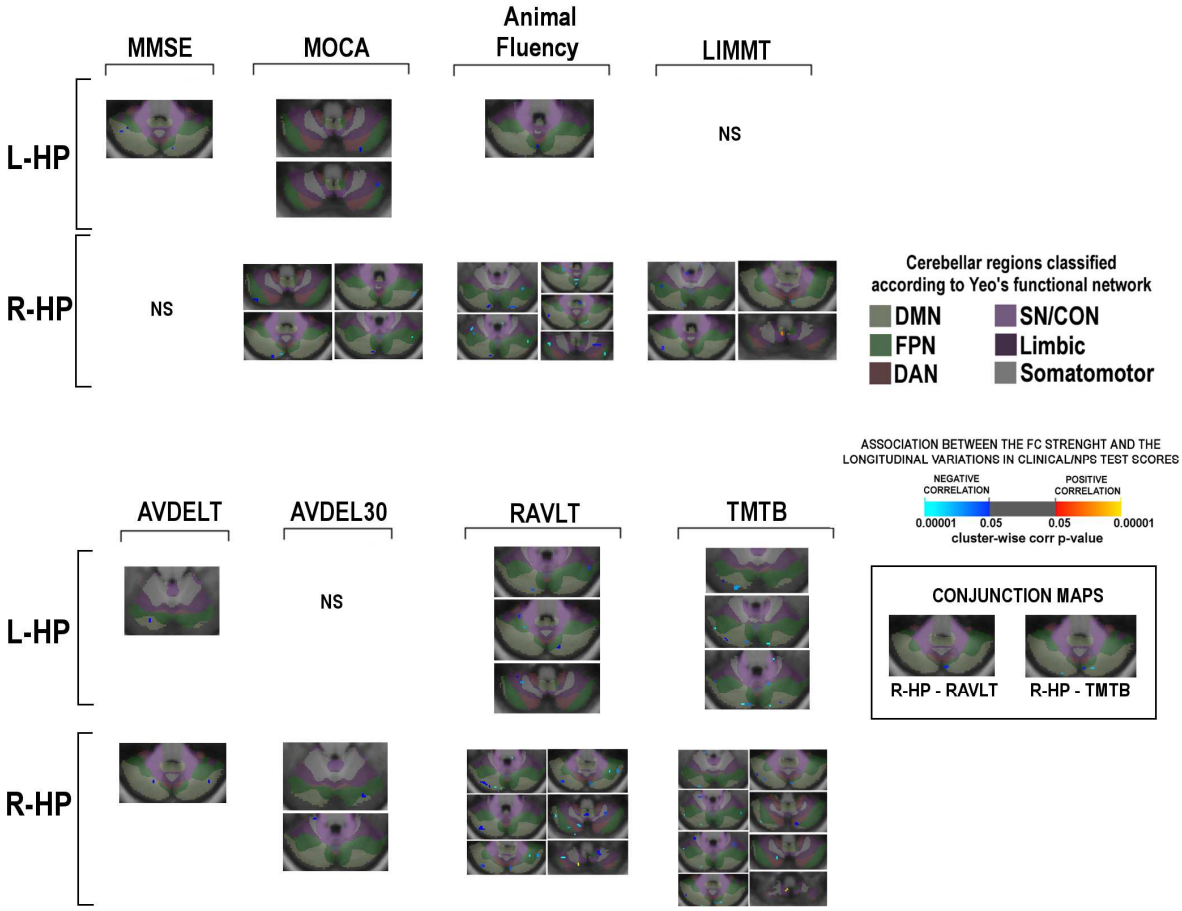

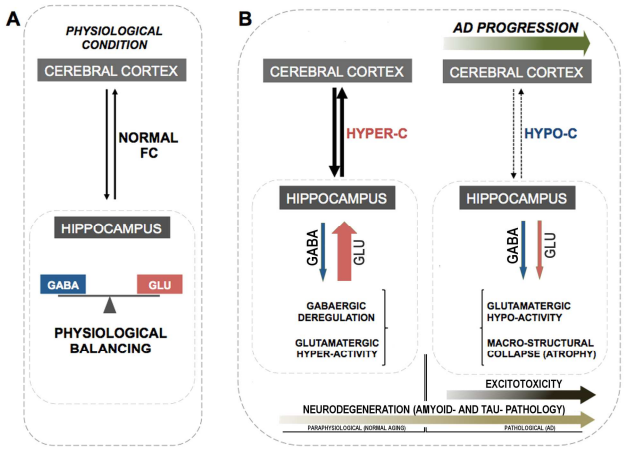

Highlights

1. AD patients display brain atrophy and hippocampal/entorhinal cortex, HP/EC, hypo-connectivity
2. Non-converting MCI subjects or MCI with no AD-related pathology, nc-MCI/MCI^{AD-}, do not show signs of cortical atrophy
3. Converting MCI patients or MCI with signs of AD-related pathology, c-MCI/MCI^{AD+}, show HP/EC hypoconnectivity along with memory deficits
4. nc-MCI/MCI^{AD-} subjects show HP/EC hyper-connectivity and preserved cognition
5. The hyperconnectivity of nc-MCI/ MCI^{AD-} may serve a compensatory role